ETH zürich

MaP | Competence Center for Materials and Processes

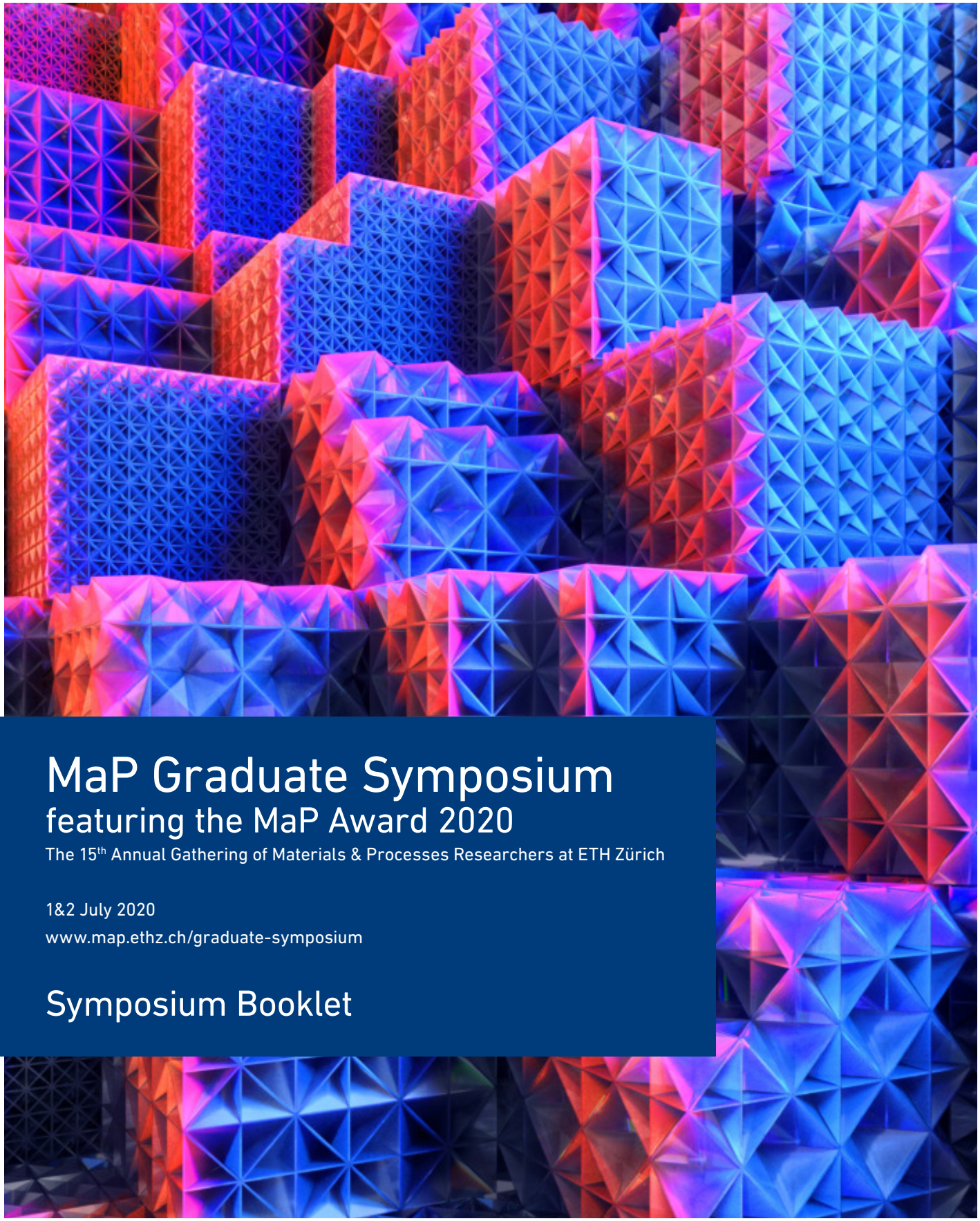

MaP Graduate Symposium

featuring the MaP Award 2020

The 15th Annual Gathering of Materials & Processes Researchers at ETH Zürich

1&2 July 2020

www.map.ethz.ch/graduate-symposium

Symposium Booklet

MaP Competence Center for Materials and Processes

MANY THANKS TO OUR SPONSORS!

TABLE OF CONTENTS

PROGRAM 3

WEDNESDAY 01 JULY 2020 3

THURSDAY 02 JULY 2020 4

ABSTRACTS OF TALKS 5

SESSION 1: 01 JULY 2020, 13.15 – 14.15 5

MAP AWARD 2020: 01 JULY 2020, 14.25 – 15.25 8

SESSION 2: 02 JULY 2020, 09.05 – 10.05 10

SESSION 3: 02 JULY 2020, 10.35 – 11.35 13

POSTER PRESENTATIONS 16

ABSTRACTS OF POSTERS 19

ADDITIVE MANUFACTURING 19

BIOLOGY, DRUG DELIVERY & TISSUE ENGINEERING 20

BIOMATERIAL DESIGN & CHARACTERIZATION 23

COMPOSITE STRUCTURES 27

ENERGY, ELECTRONICS & DEVICES 28

INORGANIC CHEMISTRY & NANOCRYSTAL DESIGN 30

LIQUID PHASES & POLYMERS 32

MAGNETICS 34

MECHANICAL PROPERTIES OF SOLIDS 35

OPTICS, PHOTONICS & PLASMONICS 39

THIN FILMS & MESOSCOPIC STRUCTURES 42

PROGRAM

Wednesday 01 July 2020

13.00	**Opening remarks**
13.15	**Bruno Marco-Dufort,** *Macromolecular Engineering, D-MAVT* Design of Dynamic Biomaterials for Thermal Stabilisation of Biologics
13.28	**Claudius Dietsche,** *Bioanalytics, D-BSSE* Deterministic Co-encapsulation of Beads and Cells in nL-droplets for High Throughput Multiplexed Single-cell Analysis
13.41	**Dr. Joydeb Mandal,** *Surface Science & Technology, D-MATL* Impact of Dispersity and Hydrogen Bonding on the Lubricity of Poly(acrylamide) Brushes
13.54	**Nicole Aegerter,** *Composite Materials & Adaptive Structures, D-MAVT* Pultrusion of Novel Fiber-reinforced Thermoplastic Composite Intermediate Materials
14.07	**MaP Mastermind** Quiz #1
14.15	*Break*
MaP Award 2020	
14.25	**Dr. Felix Eltes,** *Multifunctional Ferroic Material, D-MATL* Barium Titanate Pockels Modulators Integrated With Silicon Photonic Circuits
14.45	**Dr. Flavia Timpu,** *Optical Nanomaterial Group, D-PHYS* Linear and Nonlinear Optics With Metal Oxides: From Single Nanoparticles to Metasurfaces
15.05	**Dr. Lucas Armbrecht,** *Bioanalytics, D-BSSE* Microfluidics for Functional Analysis of Circulating Tumor Cells
15.25	**Poster Session**
16.00	*Break*
16.10	**Round Tables**
17.00	**Award Ceremony** Image Contest, Industry Poster Awards, MaP Award
17.15	**Closing & MaP Mixer**
17.45	End of Symposium Day 1

Thursday 02 July 2020

09.00	**Opening remarks**
09.05	**Julian Koch,** *Functional Materials, D-CHAB* A DNA-of-things Storage Architecture to Create Materials with Embedded Memory
09.18	**Aniket Sandip Mule,** *Optical Materials Engineering, D-MAVT* How Magic-sized Clusters Grow: Insights from Experiments
09.31	**Dr. Nako Nakatsuka,** *Biosensors & Bioelectronics, D-ITET* DNA Aptamer-functionalized Quartz Nanopipettes for Serotonin Sensing from Neurons
09.44	**Remo Schäppi,** *Renewable Energy Carriers, D-MAVT* Methanol from Sunlight and Air Using a Modular Solar Dish Reactor System
09.57	**MaP Mastermind** Quiz #2
10.05	**Flash Poster Presentations**
10.20	*Break*
10.30	**Tommaso Magrini,** *Complex Materials, D-MATL* Bioinspired Functional Composites: Transparent, Strong, and Tough
10.43	**Federico Balduini,** *Materials Integration & Nanoscale Devices*, *IBM Research* An Inside View Into an Artificial Neuron: Self-heating of Vanadium Dioxide Devices
10.56	**Lukas Roder,** *Food & Soft Materials, D-HEST* Light Gold: A Colloidal Approach Using Latex Templates
11.09	**Anastasia Terzopoulou,** *Multi-Scale Robotics, D-MAVT* Metal-Organic Frameworks for Biomedical Microrobots
11.22	**MaP Mastermind** Quiz #3
11.30	*Break*
11.35	**Award Ceremony** MaP Poster Prize, People's Choice Poster Prize, & MaP Mastermind
11.50	**Closing**

ABSTRACTS OF TALKS

Session 1: 01 July 2020, 13.15 – 14.15

Chair: Prof. Maria Lukatskaya (Electrochemical Energy Systems, D-MAVT)

Design of Dynamic Biomaterials for Thermal Stabilisation of Biologics

Bruno Marco-Dufort[1], Francesco Gatti[1], David Busha[2], John R. Janczy[2], Balaji V. Sridhar[2], Mark W. Tibbitt[1]
[1] Macromolecular Engineering, D-MAVT, ETH Zurich
[2] Nanoly Bioscience Inc., Denver

Biologics, including enzymes and virus-based vaccines, are highly susceptible to thermal stresses. In order to guarantee quality and safety, biologics must be maintained within a tight temperature window (2-8 °C). Approaches to obviate the reliance on the 'cold chain' focus on biologics engineering, excipient formulation, lyophilisation, and direct encapsulation. Building on these advances, we developed a synthetic hydrogel platform for direct encapsulation and thermal stabilisation of biologics. We used boronic ester-based dynamic covalent hydrogels, where the bonds in the network can rearrange in response to external stimuli (Fig. a), enabling on-demand release of cargo through triggered dissolution in sugar-containing aqueous buffers (Fig. b) [1]. Stabilisation was initially demonstrated for a model enzyme (leucine aminopeptidase; 50 °C, Fig. c). Adenoviruses comprise an important class of biologics used in vaccine development and gene therapy. However, broad use has been limited by poor stability. We applied our platform to stabilize an adenovirus (Type 5; 65 °C, Fig. d), as a step towards protecting viral vaccines. Our approach is a simple biomaterial-based solution to protect biologics from thermal stresses and to mitigate the risks associated with reliance on a continuous cold chain.

[1] B. Marco-Dufort, et al., Mater. Today Chem. 12, 16-33 (2019).

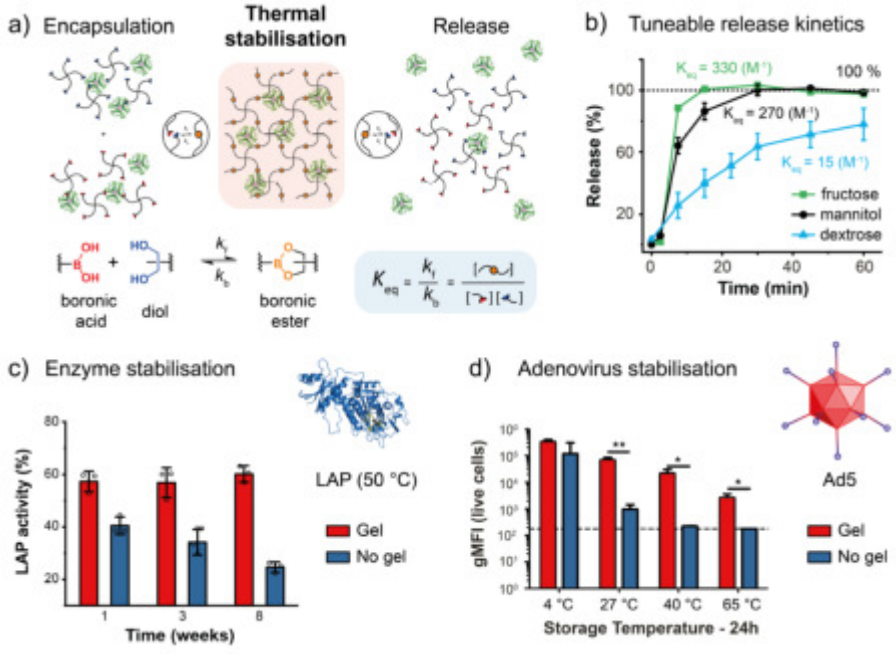

Fig.: Dynamic biomaterials enable thermal stabilisation of biologics. (a) Direct encapsulation within boronic ester-based dynamic covalent hydrogels enabled thermal stabilisation of a broad range of biologics and release on demand. (b) Release of stabilised cargo was achieved through triggered dissolution in an aqueous buffer. The binding strength (Keq) of different sugars to the boronic acids that comprise the network modulated the kinetics of release. Extensive protection against thermal stresses was demonstrated for (c) the enzyme leucine aminopeptidase (LAP) and for (d) adenovirus type 5 (Ad 5).

Deterministic Co-encapsulation of Beads and Cells in nL-droplets for High Throughput Multiplexed Single-cell Analysis

Claudius Dietsche[1], Elisabeth Hirth[1], Petra S. Dittrich[1]
[1] Bioanalytics, D-BSSE, ETH Zurich

Impact of Dispersity and Hydrogen Bonding on the Lubricity of Poly(acrylamide) Brushes

Joydeb Mandal[1], Rok Simic[1], Nicholas D. Spencer[1]
[1] Surface Science & Technology, D-MATL, ETH Zurich

The effects of chain-length dispersity and monomer type on the lubricity of acrylamide-based polymer brushes are examined in aqueous media. The polymer brushes with varying degree of chain-length dispersities, are synthesised by surface-initiated atom transfer radical polymerization (SI-ATRP) of N,N-dimethylacrylamide (DMAM), N-hydroxyethyl acrylamide (HEAM) and N-isopropylacrylamide (NIPAM)[1,2]. While an influence of the dispersity on the lubricity of the polymer brushes can be observed, it is convoluted with the competing phenomena of hydrogen bonding and increased water content. The most hydrophilic, p(HEAM) brush exhibits the highest friction coefficient (μ) of ~ 0.04 compared to ~ 0.004 in the case of the p(DMAM) brush. Such a large difference is presumed to originate from the hydrogen bonding between the tribological countersurface (plasma-oxidized PDMS) and the p(HEAM) chains, as evidenced by the substantial reduction in μ when the friction measurements are performed in 5M urea solution instead of pure milli-Q water. Interestingly, similar friction measurements in 5M urea solution for p(DMAM) and p(NIPAM) brushes, exhibited very different friction behaviour as shown in the figure. The underlying reasons for such anomalous behaviour will be discussed in the presentation.

[1] J. Mandal, et al., Polymer Chemistry, 10, 3925 (2019).
[2] N.V. Tsarevsky, et al., Macromolecules, 37, 9768 (2004).

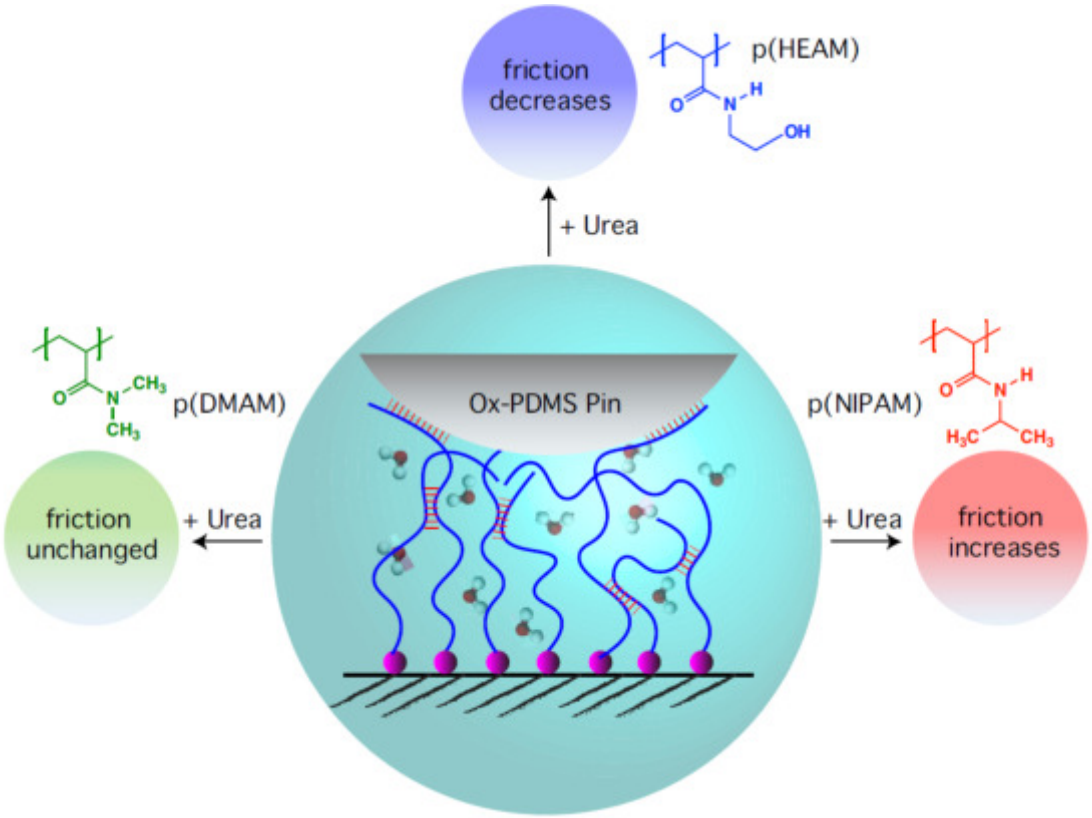

Fig.: Schematic illustration, showing the interaction between the tethered polymer chains and PDMS-countersurface and how the chemistry of the functional groups affects their frictional behaviour.

Pultrusion of Novel Fiber-reinforced Thermoplastic Composite Intermediate Materials

Nicole Aegerter[1], Maximilian Volk[1], Shelly Arreguin[1], Joanna C. Wong[2], Paolo Ermanni[1]
[1] Composite Materials & Adaptive Structures, D-MAVT, ETH Zurich
[2] Mechanical & Manufacturing Engineering, University of Calgary

Fiber-reinforced thermoplastic (TP) composites have gained traction due to their increased fracture toughness, recyclability and lack of chemical curing reactions [1]. However, their high melt viscosities requires intermediate product forms for time efficient and high-quality processing. Recently, a novel material architecture has been developed consisting of individual reinforcement fibers clad in a thermoplastic sheath, termed hybrid bicomponent fibers (BCF) [2-5]. BCF preforms overcome the processing challenges associated with current state-of-the art TP preform technologies, namely; flexibility combined with high volume manufacturing [6]. The novel BCF technology is now being explored for its application potential in small to large diameter pultruded rods. It is demonstrated that drawing BCFs with 45 to 55% fiber volume content E-glass/polycarbonate through a heated 5 mm diameter die and varying: material throughput, mold temperature and pultrusion velocities yields lower void contents when compared to state-of-the art commingled yarns. This suggests that sintering of the thermoplastic sheaths in BCF provides a superior consolidation mechanism to the otherwise flow dominated consolidation mechanism of commingled yarns [7]. This study demonstrates the potential of hybrid bicomponent fibers as a material architecture tailored for application specific technologies, which are otherwise commercially unavailable.

[1] T. Renault, 2nd International Conference & Exhibition on Thermoplastic Composites (ed. Borgmann, H.) 17–20, Bremen, Germany (2014).
[2] C. Schneeberger, et al., SAMPE Europe Conference 16, Liege, Belgium (2016).
[3] C. Schneeberger, et al., 17th European Conference on Composite Materials, Munich, Germany (2016).
[4] C. Schneeberger, et al., Composites Part A: Applied Science and Manufacturing, 103 (Supplement C), 69 (2017).
[5] C. Schneeberger, et al., 21st International Conference on Composite Materials (ICCM21), Xian, China (2017).
[6] M. Raubal, et al., SCCER Mobility Working Paper (2017).
[7] B.P. van West, et al., Polym. Compos. 12, (1991).

MaP Award 2020: 01 July 2020, 14.25 – 15.25

Chair: Prof. André Studart (Complex Materials, D-MATL)

Barium Titanate Pockels Modulators Integrated With Silicon Photonic Circuits

Felix Eltes
Multifunctional Ferroic Materials, D-MATL, ETH Zurich

Driven by the ever-increasing demands of video streaming, social media, and cloud computing, the traffic inside data centres has exploded. To cope with the increasing traffic, optical communication, which was previously only used for long-distance communication, has made its way inside data centres. The development of high-speed optical transceivers based on silicon photonic integrated circuit (Si-PIC) technology has al-lowed optical fibres to replace electrical wires for communication down to distances >1 m. Available Si-PIC platforms rely on modulators based on the plasma-dispersion effect to convert electrical signals into optical signals. However, these modulators intrinsically suffer from large power consumption and limited performance. Using the Pockels effect enables highly efficient, low-power modulators, however no such technology exists today.
We have developed a hybrid barium titanate ($BaTiO_3$)-Si photonics technology with a strong Pockels effect on large-scale silicon substrates as a platform for integrated Pockels modulators. The platform enables scalable, integrated Si-$BaTiO_3$ devices with large Pockels coefficients for electro-optic modulation. We have demonstrated the performance and scalability of the technology for communications, and how it can be exploited for novel applications such as ultra-low power tuning, and cryogenic photonics.

Linear and Nonlinear Optics With Metal Oxides: From Single Nanoparticles to Metasurfaces

Flavia Timpu
Optical Nanomaterials, D-PHYS, ETH Zurich

We propose novel strategies and materials to increase the interaction of light with matter at sizes smaller than the wavelength. We focus in particular on the second harmonic generation (SHG), which is a nonlinear optical process in which the wavelength of the light is converted to half of its value. We propose two metal ox-ides, barium titanate ($BaTiO_3$) and lithium niobate ($LiNbO_3$), which are all-dielectric materials with an extended applicability range. These two materials have large band gaps and reasonably high second order susceptibility, thus showing SHG over a broad range from the near-ultraviolet to the near-infrared range with very low losses. Additionally, nanostructures of $BaTiO_3$ and $LiNbO_3$ have high refractive indices, which make it possible to confine light in their volume and obtain resonances. We show that SHG at the nanoscale is enhanced at these intrinsic resonances. We also combine $BaTiO_3$ with plasmonic nanostructures in hybrid nanostructures, to exploit the strong field confinement outside the surfaces of plasmonic nanostructures. Finally, we use the findings about single nanostructure to design and show the integration of $BaTiO_3$ nanostructures in SHG emitting metasurfaces. We obtain nonlinear optical devices that exploit the optical properties of single nanostructures in periodic arrays to manipulate the wavefront of light over subwavelength scales.

Microfluidics for Functional Analysis of Circulating Tumor Cells

Lucas Armbrecht
Bioanalytics, D-BSSE, ETH Zurich

Cancer cells can be released from a primary tumor and migrate into blood stream, from whereon they may form metastases at distant sites of the body. Today, it is possible to infer cancer progression and treatment efficacy by determining the number of circulating tumor cells (CTCs) in the patient's blood at multiple time points. Unfortunately, further valuable information about CTC phenotypes remains inaccessible as most methods are destructive and alter cellular behaviour.
In my PhD, a microfluidic method for integrated capture, isolation, and analysis of CTCs was developed. The platform allows the use of traditional membrane markers and on top enables quantification of proteins secreted by single CTCs and CTC clusters. This is especially important as it was recently shown that CTCs can actively alter tissue behaviour to facilitate the formation of metastases. The new platform is small, cost-efficient and can isolate CTCs from whole blood with extraordinary efficiencies above 95%. We tested our platform with multiple breast cancer cell lines spiked into human blood, mouse-model-derived CTCs, and patient samples. The modular approach using magnetic particles as mobile carriers for the biological test enables scientists to measure thousands of target molecules on this platform in future and has already helped to under-stand the metastatic cascade in more detail.

Session 2: 02 July 2020, 09.05 – 10.05

Chair: Prof. Laura Heyderman (Mesoscopic Systems, D-MATL and PSI)

A DNA-of-things Storage Architecture to Create Materials with Embedded Memory

Julian Koch[1], Silvan Gantenbein[2], Kunal Masania[2], Wendelin J. Stark[1], Yaniv Erlich[3], Robert Grass[1]
[1] Functional Materials, D-CHAB, ETH Zurich
[2] Complex Materials, D-MATL, ETH Zurich
[3] Erlich Lab LLC, Raana, Israel

DNA storage offers substantial information density [1-3] and exceptional half-life [3]. We devised a 'DNA-of-things' (DoT) storage architecture to produce materials with immutable memory. In a DoT framework, DNA molecules record the data, and these molecules are then encapsulated in nanometer silica beads [4], which are fused into various materials that are used to print or cast objects in any shape. First, we applied DoT to three-dimensionally print a Stanford Bunny [5] that contained a 45 kB digital DNA blueprint for its synthesis. We synthesized five generations of the bunny, each from the memory of the previous generation without additional DNA synthesis or degradation of information. To test the scalability of DoT, we stored a 1.4 MB video in DNA in plexiglass spectacle lenses and retrieved it by excising a tiny piece of the plexiglass and sequencing the embedded DNA. DoT could be applied to store electronic health records in medical implants, to hide data in everyday objects (steganography) and to manufacture objects containing their own blueprint. It may also facilitate the development of self-replicating machines.

[1] G.M. Church et al., Science 337, 1628 (2012).
[2] N. Goldman, et al., Nature 494, 77 (2013).
[3] R.N. Grass, et al., Angew. Chem. Int. Ed. 54, 2552 (2015).
[4] D. Paunescu, et al., Nat. Protoc. 8, 2440 (2013).
[5] G. Turk, et al., Proc. 21st Annual Conference on Computer Graphics and Interactive Techniques, 311 (1994).

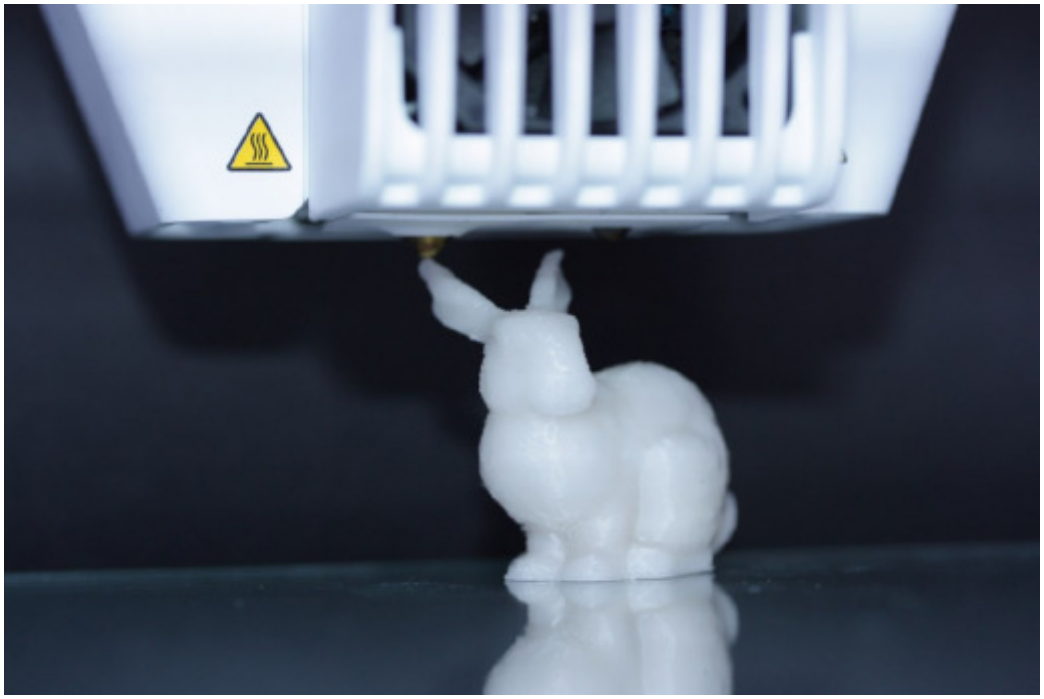

Fig.: Stanford Bunny printed with filament containing its .stl file in form of DNA.

How Magic-sized Clusters Grow: Insights from Experiments

Aniket S. Mule[1], Sergio Mazzotti[1], Aurelio Rossinelli[1], Marianne Aellen[1], Paul T. Prins[2], J.C. (Annelies) van der Bok[2], Simon F. Solari[1], Priyank V. Kumar[3], Andreas Riedinger[4], David J. Norris[1]

[1] Optical Materials Engineering, D-MAVT, ETH Zurich

[2] Debye Institute for Nanomaterials Science,Utrecht University

[3] Department of Chemical Engineering, University of New South Wales, Sydney

[4] Max Planck Institute for Polymer Research, Mainz

Magic-sized clusters (MSCs) are semiconductor nanocrystals that have well-defined structural and optoelectronic properties. These clusters are believed to grow in discrete steps from one “magic” size to the next. However, even after decades of study, the nanocrystal community does not have a detailed understanding of why “magic” sizes exist and how they grow. This is due in part to the challenges in their experimental investigation, e.g. due to their small size they can be difficult to isolate and image via electron microscopy. Here, we work to overcome these issues by developing a synthetic protocol that yields MSCs up to larger length scales. These particles can be isolated and purified easily using size-selective precipitation. We then analyse a series of these MSCs using a combination of optical (absorption, photoluminescence, and photoluminescence excitation) and structural characterisation (XRD, NMR, and TEM). The comparison of these results with previous reports suggests that the particles exhibit tetrahedral shapes. Based on our observations, we propose an atomistic model that explains the growth of MSCs and rationalizes the existence of their precise structures. This work improves our understanding of nanocrystal growth and could help expand the library of available MSCs.

DNA Aptamer-functionalized Quartz Nanopipettes for Serotonin Sensing from Neurons

Nako Nakatsuka[1], Alix Faillétaz[1], Krishna C. Vadodaria[2], Dominic Eggemann[1], Fred H. Gage[2], János Vörös[1], Dmitry Momotenko[1]

[1] Biosensors & Bioelectronics, D-ITET, ETH Zurich

[2] Laboratory of Genetics, Salk Institute for Biological Studies, La Jolla

Advancing our understanding of neuronal communication necessitates biochemical sensors that approach the spatial resolution of chemical signaling via neurotransmitters at synapses that span only ca. 20 nm across. We have developed artificial nanopores in the form of quartz nanopipettes with 10 nm orifices functionalized with molecular recognition elements termed aptamers. Aptamers are systematically designed oligonucleotide receptors that exhibit highly specific and selective recognition of targets such as serotonin [1]. Nanoscale confinement of ion fluxes, analyte-specific changes in molecular conformation of aptamer species, and related surface charge variations enable specific and selective serotonin sensing . We demonstrated the capacity to detect physiologically relevant differences in serotonin amounts in complex media collected from human induced pluripotent stem cell-derived serotonergic neuron cultures [2]. Human serotonergic neurons treated with the antidepressant and selective serotonin reuptake inhibitor, Citalopram, or exposed to KCl that triggers neuronal depolarization, exhibited higher serotonin release into the extracellular media. By interrogating the sensing mechanism and validating detection in clinically relevant samples, we demonstrate the potential of conformationally changing aptamer-modified nanopipettes as a rapid, label-free, and translatable nanotool for diverse biological systems.

[1] N. Nakatsuka, et. al., Science 362, 319 (2018).

[2] K.C. Vadodaria, et. al., Mol. Psychiatry, 24, 808 (2019).

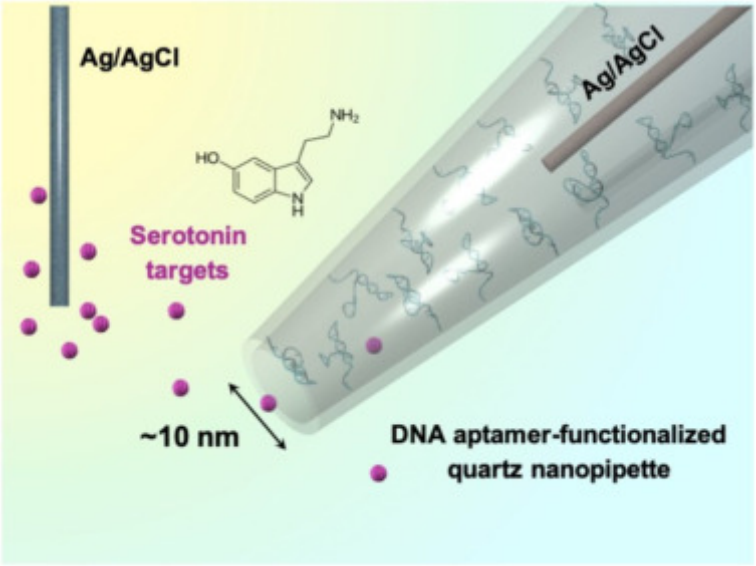

Fig.: Schematic of DNA aptamer-functionalized quartz nanopipettes. The current is measured between two Ag/AgCl quasi-reference counter electrodes, one inside the nanopipette and the other in the bulk solution. Flux of serotonin targets through the ~10 nm opening of the nanopipette is transduced as a change in current response due to aptamer conformational rearrangement upon target recognition, which alters the ionic permeability inside the nanopipette.

Methanol from Sunlight and Air Using a Modular Solar Dish Reactor System

Remo Schäppi[1], David Rutz[1], Philipp Haueter[1], Philipp Furler[1,2], Aldo Steinfeld[1]
[1] Renewable Energy Carriers, D-MAVT, ETH Zurich
[2] Synhelion SA, Lugano

We report on the experimental pilot demonstration of a modular solar dish-reactor system for the production of methanol from ambient air using concentrated solar energy. We describe the complete process chain and its key components, and present representative on-sun runs with fully-automated consecutive CO_2-splitting and H_2O-splitting redox cycles. The system integrates three thermochemical units operated in series, namely: 1) the capture of CO_2 and H_2O directly from ambient air via an adsorption-desorption cyclic process; 2) the co-splitting of CO_2 and H_2O to generate a specific mixture of CO and H_2 (syngas) via a reduction-oxidation cyclic process using concentrated solar energy; and, 3) the gas-to-liquid synthesis of methanol. The experimental validation of the entire process chain to solar methanol under realistic field conditions was accomplished by moving from a laboratory setup [1] to a modular solar system [2], thereby advancing the technological readiness and its industrial implementation. The solar reactor for effecting this redox cycle consists of a cavity-receiver containing a reticulated porous ceramic (RPC) foam structure made of pure CeO_2. The RPC is directly exposed to the high-flux solar intensity and provides efficient radiant absorption and combined heat/mass transport within the reaction site. Two identical solar reactors are mounted side-by-side on a solar concentrator subsystem [2]. Downstream of the two solar reactors, the syngas is compressed and subsequently processed to methanol in a catalytic gas-to-liquid packed-bed reactor. Fully automatized full day on-sun consecutive cycles demonstrate the stability and robustness of the system. Solar runs with varying H_2O/CO_2 mixtures further show the flexibility of the system to produce syngas in the desired quality and stoichiometry suitable for the downstream gas-to-liquid process, e.g. Fischer-Tropsch or methanol synthesis.

[1] D. Marxer, et. al., Energy Environ. Sci. 10, 1142 (2017).
[2] F. Dähler, et. al., Solar Energy 170, 568 (2018).

Session 3: 02 July 2020, 10.35 – 11.35

Chair: Prof. Dennis Kochmann (Mechanics & Materials, D-MAVT)

Bioinspired Functional Composites: Transparent, Strong, and Tough

Tommaso Magrini[1], Florian Bouville[2], Alessandro Lauria[3], André R. Studart[1]
[1] Complex Materials, D-MATL, ETH Zurich
[2] CASC, Department of Materials, Imperial College London
[3] Multifunctional Materials, D-MATL, ETH Zurich

Materials combining optical transparency and mechanical strength are highly demanded for electronic displays, structural windows and in the arts, but the oxide-based glasses currently used in most of these applications suffer from brittle fracture and low crack tolerance. We have developed a simple and scalable processing route to fabricate bulk transparent composites with a brick-and-mortar architecture inspired by seashells that can effectively slow down the propagation of cracks during fracture of the silica-based material [1]. The relative improvement in optical transmission between the porous glass scaffold and the final composite is striking, especially when the materials are placed on top of a retro-illuminated pattern, such as a smartphone screen (Fig. 1a). To achieve optical transparency in this brick-and-mortar microstructure, we infiltrate the percolating network of glass platelets (the bricks) with a refractive-index-matching polymer matrix (the mortar). Mechanical characterization shows that our bioinspired glass composites are up to 3-fold tougher than common glasses, while keeping flexural strengths that are comparable to transparent polymers, silica- and other conventional glasses. The high fracture resistance of the composites arises from the interplay of several extrinsic toughening mechanisms, namely crack deflection, polymer bridging and platelet pullout (Fig. 1b). Furthermore, the stiff reinforcing glass platelets provide the composite with hardness levels that are one order of magnitude higher than that of transparent polymers. In summary, this study demonstrates that implementing biological design principles into glass-based materials at the microscale opens a promising new avenue for the manufacturing of structural bioinspired materials combining antagonistic functional properties.

[1] T. Magrini, et. al., Nature Communications 10, 2794 (2019).

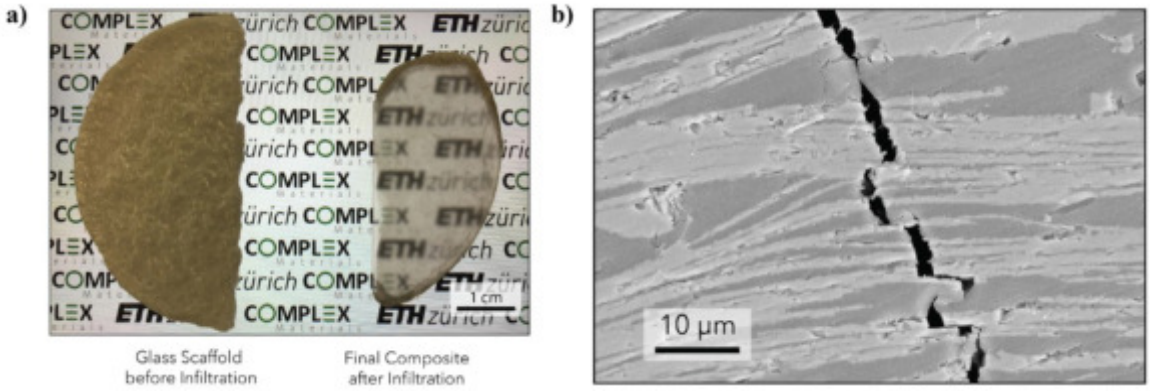

Fig.: a) Nacre-like composite before and after infiltration. Effect of the infiltration of a refractive index matching polymer in a porous glass scaffold (left), resulting in a 2-mm thick bioinspired transparent composite (right). Picture taken from a sample placed on top of a smartphone screen (retro-illuminated). b) Scanning electron micrograph highlighting the fracture path within the composite.

An Inside View Into an Artificial Neuron: Self-heating of Vanadium Dioxide Devices

Federico Balduini[1], Elisabetta Corti[1], Joaquin Antonio Cornejo Jimenez[1], Kirsten Moselund[1], Siegfried Karg[1], Bernd Gotsmann[1]
[1] IBM Research Zurich

Vanadium dioxide is a phase change material in which the metal-to-insulator transition can be triggered by self-heating of electrically activated devices [1]. Such property makes VO_2 a suitable material for application ranging from thermal sensors and optical devices to neuromorphic computing devices. The investigation of the VO_2 phase transition induced by self-heating, therefore would benefit the understanding of MIT modulation for such applications. Previous research shows that the insulator-to-metal transition in crystalline samples happens through a filamentary formation of the metallic phase. However, still little is known about the formation of the metallic phase in polycrystalline and granular films, such as films prepared on a Silicon substrate for CMOS compatibility. In this work we present thermal characterization of VO_2 on Si/SiO_2 devices for Oscillatory Neural Network application performed using Scanning Thermal Microscopy (SThM). With SThM imaging, we measure the temperature profile of the phase transition in an activated device with nm resolution, highlighting the borders between metallic and insulating VO_2 grains and the power distribution in the metallic grains. Thereby the current path can be reconstructed. A model based on thermally induced phase transition due to Joule heating can reproduce the experimental observation and the IV characteristic of this device.

[1] H. Kim, et al. New J. Phys. 6, 52 (2004).

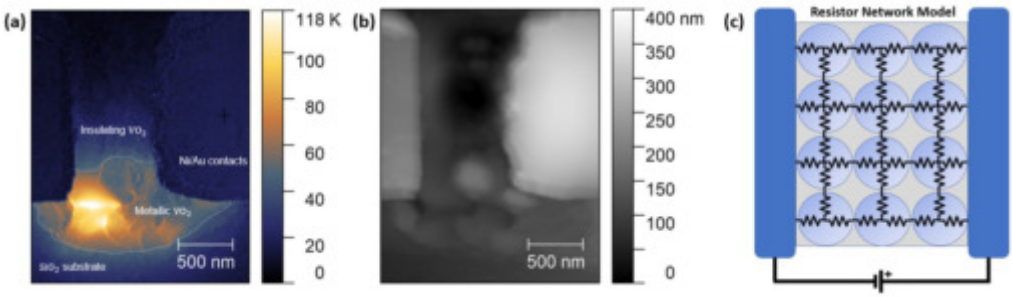

Fig.: (a) Temperature map and (b) topography of a self-heated VO_2 device obtained using scanning thermal microscopy. A hot spot is indicative of current crowding through a single grain. Further analysis is based on modelling generation and conduction of Joule in the self-heating grains. This enables assigning the current path through device. The insight feeds into a (c) resistor network model analysing the formation of current paths in grainy, self-heated films.

Light Gold: A Colloidal Approach Using Latex Templates

Lukas E. Roder[1], Leonie van 't Hag[1], Raffaele Mezzenga[1]
[1] Food & Soft Materials, D-HEST, ETH Zurich

A new 18 karat light gold, composed of gold single crystals, amyloids, and a polymer latex matrix is developed. It is similar to a glassy plastic, yet lighter than aluminum and of use in watches, jewelry, radiation shielding, catalysis, and electronics. The material is prepared via a hydrogel precursor dried into an aerogel. Annealing of the polystyrene matrix under vacuum gives rise
to a homogeneous template. The final apparent density and porosity of the material depend directly on the volumetric concentration of the starting solution used for hydrogel formation. After annealing, a homogeneous micro- structure is obtained in which the shining gold single crystal platelets are evenly embedded in a polystyrene matrix. The material has a glass transition temperature of ≈105 °C, which allows for annealing and molding above this temperature. A general scaling behavior is found for the Young's modulus of the material with the density. The Young's modulus of the material with a density of 1.7 g cm^{-3} is ≈50 MPa. The density and stiffness, as well as the color, of the material can be tuned depending on the final application [1,2].

[1] L. van 't Hag, et. al., Adv. Funct. Mater. 30, 1908458 (2020).
[2] J.R. Smith, et. al., Phys. Rev. Lett. 57, 671 (2016).

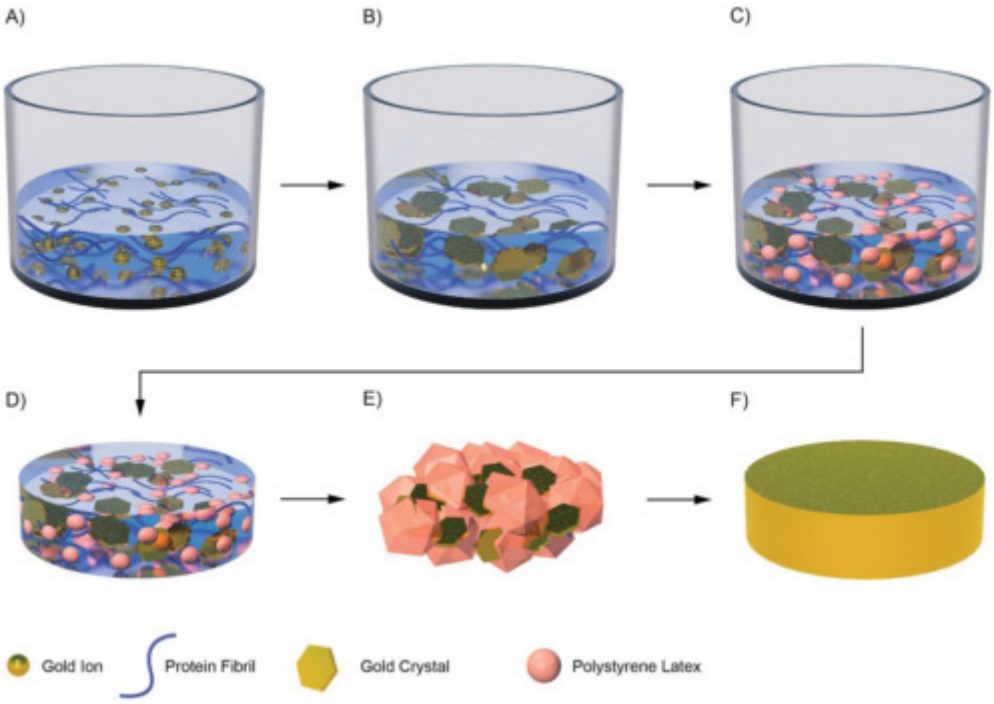

Fig.: Illustration of the light gold production process. A) A mixture of BLG fibrils and gold ions forms B) gold single crystals upon incubation at 60 °C for 16 h. C) Colloidal polystyrene latex is added into the solution before D) hydrogel formation upon the diffusion of NaCl through a membrane. E) Supercritical CO_2 drying (upon solvent exchange: aqueous solution for ethanol) results in the formation of a robust gold aerogel. F) Annealing of the polystyrene latex above its glass transition temperature of 100–105 °C results in a transparent matrix for the gold crystals.

Metal – Organic Frameworks for Biomedical Microrobots

Anastasia Terzopoulou[1,3], Xiaopu Wang[2], Xiang-Zhong Chen[1], Salvador Pané[1], Josep Puigmartí-Luis[3]
[1] Materials for Robotics, D-MAVT, ETH Zurich
[2] Multi-Scale Robotics, D-MAVT, ETH Zurich
[3] Biochemical Engineering, D-CHAB, ETH Zurich

POSTER PRESENTATIONS

Name	Poster Title	Affiliation
Marianne **Aellen**	Revisiting Design Principles of 2D Metallic Lasers: Coexistence and Competition of Plasmonic and Photonic Modes	Optical Materials Engineering, D-MAVT
Cameron **Boggon**	Capillary-Assisted Deposition of Bacteria as a Tool for Studying Population Heterogeneity	Soft Materials & Interfaces, D-MATL
Xiang-Zhong **Chen**	Hybrid Magnetoelectric Microrobots for Biomedical Applications	Multi-Scale Robotics, D-MAVT
Ming **Chen**	Probing the Limits of Strength in Diamonds: From Single- and Nano-crystalline to Diamond-like-carbon (DLC)	Nanometallurgy, D-MATL
Jasper **Clarysse**	Size and Composition Controlled Intermetallic Nanocrystals via Amalgamation Seeded Growth	Materials & Device Engineering, D-ITET
Ario **Cocina**	A Local-density-of-optical-states Approach to Excited-state Dynamics of Colloidal Semiconductor Nanocrystals	Optical Materials Engineering, D-MAVT
Elisabetta **Corti**	Grain-size Tuning of VO_2 Films on Si Using Millisecond Flash Annealing	NANOLAB, EFPL
Madeleine **Fellner**	Transparent Nacre-inspired Composite Materials	Multifunctional Materials, D-MATL
Sara **Fiore**	Ab initio Modeling of Thermal Transport through van der Waals Materials	Computational Nanoelectronics, D-ITET
Alexander **Firlus**	Atomic-scale Investigations of the Invar Effect in Fe-based Bulk Metallic Glasses	Metal Physics & Technology, D-MATL
Dominic **Gerber**	Why Does Freezing Cause so Much Damage?	Soft & Living Materials, D-MATL
Caroline **Giacomin**	Particle Laden Porcine Gastric Mucin Strength	Food Process Engineering, D-HEST
Michael **Grimes**	Non-resonant Magnetic X-ray Diffraction to Monitor the Quenching of Anti-ferromagnetic Order of FeRh Films	Mesoscopic Systems, D-MATL & Paul Scherrer Institut (PSI)
Hongri **Gu**	Magnetic Quadrupole Assemblies with Arbitrary Shapes and Magnetizations	Multi-Scale Robotics, D-MAVT
Linos **Hecht**	Two-Color Diffraction Imaging of Helium Nanodroplets	Nanostructures & Ultrafast X-Ray Science, D-PHYS
Kevin **Hofhuis**	Thermally Superactive Nanomagnets Obtained with Interfacial Dzyaloshinskii-Moriya Interaction	Mesoscopic Systems, D-MATL & Paul Scherrer Institut (PSI)
Maximilian **Jansen**	Investigating Long Range Vibrations in Nanocrystal Solids	Materials & Device Engineering, D-ITET
Petra **Juskova**	Addressable Microfluidic Platform for Cultivation and Monitoring of Individual Microbial Cells	Bioanalytics, D-BSSE
Robert **Keitel**	Photoluminescence Excitation Spectroscopy on Individual Quantum Emitters	Optical Materials Engineering, D-MAVT

Nicole **Kleger**	3D Printing of Salt Templates for Magnesium with Complex Porosity	Complex Materials, D-MATL
André **Kling**	Rapid Prototyping and Multiplexed Surface Functionalization of Thermoplastic Lab-on-chip Devices	Bioanalytics, D-BSSE
Katharina **Kolatzki**	Setup and Characterization of a Helium Liquid Jet for Diffraction Experiments	Nanostructures & Ultrafast X-Ray Science, D-PHYS
Junggou **Kwon**	Nitrogen Doped TiO_2 Nanoparticle-based Aerogels for Visible-light-driven Photocatalytic H_2 Production	Multifunctional Materials, D-MATL
Nolan **Lassaline**	Optical Fourier Surfaces	Optical Materials Engineering, D-MAVT
Seunghun **Lee**	A Biomimetic Macroporous Hybrid Scaffold with Sustained Drug Delivery for Enhanced Bone Regeneration	Orthopaedic Technology, D-HEST
Zhentao **Liu**	Epitaxial Growth and Electrical Control of Antiferromagnetic Mn_2Au Films	Mesoscopic Systems, D-MATL & Paul Scherrer Institut (PSI)
Byron **Llerena Zambrano**	Magnetic Alignment of Nanowires for Next Generation Stretchable Electronics	Biosensors & Bioelectronics, D-ITET
Ines **Lüchtefeld**	Towards the Fluorescent Investigation of Spatiotemporal Membrane Tension Changes in Biological Membranes During Micromanipulation	Biosensors & Bioelectronics, D-ITET
Sergio **Mazzotti**	How Magic-Sized Clusters Grow: A Microscopic Theory	Optical Materials Engineering, D-MAVT
Andrea **Morandi**	Disordered Assemblies of $LiNbO_3$ Nanoparticles for SHG in Multiple Scattering Regime	Optical Nanomaterial Group, D-PHYS
Annina **Moser**	Amide-Promoted Synthesis of $AgSbTe_2$ and $Ag_xSb_{1-x}Te_{1.5-x}$ Nanocrystals	Materials & Device Engineering, D-ITET
Nako **Nakatsuka**	DNA Aptamer-functionalized Quartz Nanopipettes for Serotonin Sensing from Neurons	Biosensors & Bioelectronics, D-ITET
Aleksandra **Pac**	Ferromagnetic Heterostructures for Unconventional Computing	Mesoscopic Systems, D-MATL & Paul Scherrer Institut (PSI)
Andrew **Pun**	Strategies for Enhancing the Photolumniescence of CdSe Magic-Sized Clusters	Optical Materials Engineering, D-MAVT
Xiao-Hua **Qin**	Subtractive 3D Laser Microprinting of Cell Guidance Cues in Hydrogels	Bone Biomechanics, D-HEST
Manon **Rolland**	Effect of Polymerization Components on Oxygen-Tolerant Photo-ATRP	Polymeric Materials, D-MATL
Mario **Saucedo-Espinosa**	In-droplet Electrophoretic Separations using Carbon-based Electrodes	Bioanalytics Group, D-BSSE
Christina **Sauter**	Lithium Ion Battery Separators: The Influence of Separator Structure on Battery Performance	Materials & Device Engineering, D-ITET

Til **Schlotter**	AFM Integrated Nanopores for Single-Cell Secretomics	Biosensors & Bioelectronics, D-ITET
Rajalakshmi **Senthil Arumugam**	Comparative Studies on $LiNi_{0.5}Mn_{0.5-x}Co_xO_2$ Cathode Materials	Materials & Device Engineering, D-ITET
Sam **Treves**	Skyrmion Imaging With NV Spectroscopy and X-ray Tomography	Mesoscopic Systems, D-MATL & Paul Scherrer Institut (PSI)
Maximilian **Volk**	High Voltage Insulators Based on Pultruded Thermoplastic Composite Cores	Composite Materials & Adaptive Structures, D-MAVT
Marius **Wagner**	Feedstock Defelpment for 3D Printing of 316L Steel and Characterization of Final Material Properties	Nanometallurgy, D-MATL
Laura **Wiest**	Droplet Breakup of High-viscosity-ratio Emulsions with an Optimized Interaction Chamber	Food Process Engineering, D-HEST
Suiying **Ye**	Tuning Molecular Fluorescence in Aggregated State via Polymerization-Mediated Charge Transfer	Drug Formulation & Delivery, D-CHAB
Tao **Zhou**	Efficient Asymmetric Synthesis of Carbohydrates by Aldolase Nano-confined in Lipidic Cubic Mesophases	Food & Soft Materials, D-HEST
Jingyuan **Zhou**	Precessional Dynamics in Antiferromagnetically Coupled Ferromagnetic Films	Mesoscopic Systems, D-MATL & Paul Scherrer Institut (PSI)

ABSTRACTS OF POSTERS

Additive Manufacturing

Feedstock Defelpment for 3D Printing of 316L Steel and Characterization of Final Material Properties

Marius Wagner[1], Tutu Sebastian[2], Frank Clemens[2], Jeffrey M. Wheeler[1], Zhujun Wang[3], Marc Willinger[3], Anja Rusch[1], Rabea Ganz[1], Ralph Spolenak[1]
[1] Nanometallurgy, D-MATL, ETH Zurich
[2] High Performance Ceramics, Functional Materials, Empa
[3] ScopeM, ETH Zurich

Additive manufacturing of metals using fused deposition of metal-polymer feedstock is gaining increasing interest from research and industry (see Fig.). The composition of the polymeric binder is of major importance in this process and needs the meet complex requirements. In this work, we demonstrate a novel binder, which can be extruded into filaments and allows printing on commercial machines with high resolution. Printability is improved by decreasing the viscosity and increasing the stiffness of the binder. We demonstrate this for several 316L stainless steel feedstocks. The thermal binder removal, which is performed before the sintering, is investigated using in-situ environmental scanning electron microscopy. Sintered specimens exhibit both intra- and inter-layer porosity. Nanoindentation mapping is performed to characterize the hardness and modulus of the material. The observed properties coincide well with literature. Interestingly, the indentation experiments reveal hidden porosity. Further study is needed to assess the potential of nanoindentation as a tool for the investigation of porosity.

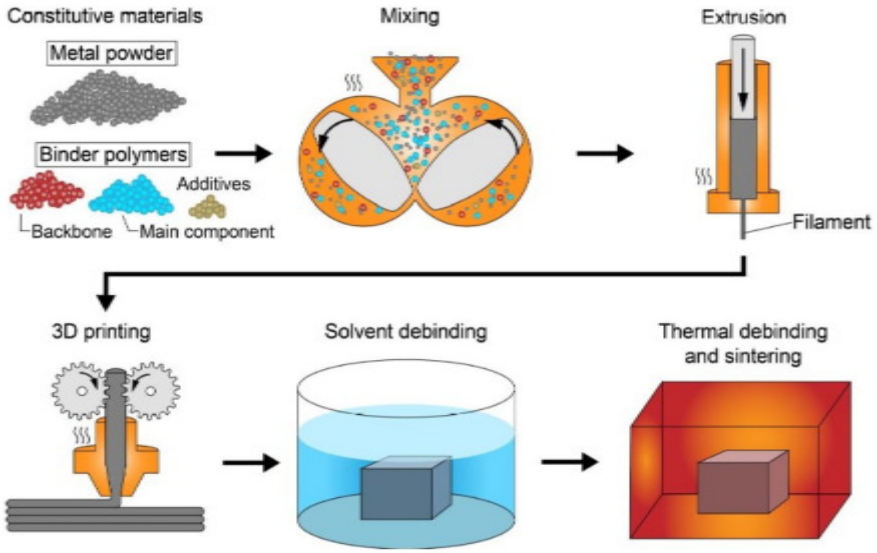

Fig.: Schematic of the fused deposition of metals process.

Subtractive 3D Laser Microprinting of Cell Guidance Cues in Hydrogels

Christian Gehre[1], Ximena Sutter[1], Philipp Campos[1], Xiaopu Wang[2], Siyu Deng[2], Bradley Nelson[2], Ralph Müller[1], Xiao-Hua Qin[1]
[1] Bone Biomechanics, D-HEST, ETH Zurich
[2] Multi-Scale Robotics D-MAVT, ETH Zurich

3D Printing of Salt Templates for Magnesium with Complex Porosity

Nicole Kleger[1], Martina Cihova[2], Kunal Masania[3], Jörg F. Löffler[2], André R. Studart[1]
[1] Complex Materials, D-MATL, ETH Zurich
[2] Metal Physics & Technology, D-MATL, ETH Zurich
[3] Faculty of Aerospace Engineering, Delft University of Technology

Porosity is an essential feature in a broad range of applications that require light-weight materials or structures with high surface area [1-3]. Natural materials also take advantage of porosity to tune the density of a material across an object, hence allowing for a wide range of material properties within one structure [4]. Porous materials can be fabricated across a vast range of materials using the salt-leaching technique [5]. However, this technique has so far been limited to the generation of random porosity with only minimal control of pore shape, size and location. We now developed a technique that combines the ease of salt leaching with the complex shape flexibility of additive manufacturing (AM) [6]. A rheologically engineered salt-based paste is 3D printed by direct ink writing into grid-like structures, thereby displaying structured porosity that spans from the submillimeter to the macroscopic scale. As a proof of concept, the obtained dried and sintered NaCl templates were infiltrated with magnesium (Mg), a metal which is difficult to process directly by AM due to its high vapor pressure and highly oxidative nature [7]. The resulting Mg scaffolds display a controlled and variable pore structure, which further allows to vary the density across the scaffold. The tunable mechanical and bioresorbable properties resulting from the control of density and surface area make these Mg structures attractive for biomedical implant applications and demonstrate the potential of this technique.

[1] L. Ma, et al., Biomaterials 24, 4833 (2003).
[2] S.P. Low, et al., Biomaterials 30, 2873 (2009).
[3] T.A. Schaedler, et al., Ann. Rev. Mater. Res. 46, 187 (2016).
[4] P. Fratzl, et al., Prog. Mater. Sci. 52, 1263 (2007).
[5] Y. Conde, et al., Adv. Eng. Mater. 8, 795 (2006).
[6] N. Kleger, et al., Adv. Mater. 31, 1337 (2019).
[7] K. Lietaert, et al., J. Magnes. Alloy. 1, 303 (2013).

Biology, Drug delivery & Tissue Engineering

Efficient Asymmetric Synthesis of Carbohydrates by Aldolase Nano-confined in Lipidic Cubic Mesophases

Tao Zhou[1], Jijo J. Vallooran[1,2], Salvatore Assenza[1], Anna Szekrenyi[3], Pere Clapés[3], Raffaele Mezzenga[1]
[1] Food & Soft Materials, D-HEST, ETH Zurich
[2] Department of Chemistry, University of Zurich
[3] Biotransformation & Bioactive Molecules, Instituto de Química Avanzada de Cataluña, Barcelona

Class-I aldolases are known for efficiently catalysing stereo-selective aldol-addition reactions in bulk aqueous media and considerable efforts are currently being devoted to engineer the enzyme in order to optimize its activity and stability, primarily by modulating the hydrophobicity of the catalytic active site. Here, we opt for a different strategy based on choosing a nano-confined environment favourable to the enzyme. We report the observation of enhanced activity and stability of a class-I aldolase, D-fructose-6-phosphate aldolase from E. coli (FSA) when incorporated into lipidic cubic mesophases (LCMs), a class of biomimetic amphiphilic complex fluids employed in several nanotechnology applications. We infer that this improved in-meso performance is achieved by optimal location of the FSA in the LCMs, as a result of the known interaction between the residues of FSA and the glycerol molecules, which serve as the lipid head groups, and thus locate along the amphiphilic interface encompassing the whole LCM. This continuous interface ensures increased accessibility of the catalytic reaction centre to substrates and high activity in LCM.

[1] T. Zhou, et. al., ACS Catal. 8, 5810 (2018).

Capillary-Assisted Deposition of Bacteria as a Tool for Studying Population Heterogeneity

Cameron Boggon[1], Clement Vulin[2], Eleonora Secchi[3], Lucio Isa[1]
[1] Soft Materials & Interfaces, D-MATL, ETH Zurich
[2] Infectious Diseases & Hospital Epidemiology, University Hospital Zurich
[3] Groundwater & Hydromechanics, D-BAUG, ETH Zurich

A range of studies have established that cultures of bacteria display heterogeneity in behaviour [1]. Examples include stochastic variation in cell size and gene expression, 'division of labour' in biofilm growth [2] and the existence of slow growing cells, known as 'persisters', that can survive toxic levels of antibiotics despite lacking any genetic immunity to the drug [3]. Understanding how cell populations differentiate and interact at the community level is increasingly seen to be critical to our understanding of infection mechanisms and the development of novel treatments. To study these systems, we need tools that allow us to image populations of bacteria with single-cell resolution. Here we present a method, based on Capillary-Assisted Particle Assembly (CAPA) [4], for immobilising populations of bacteria onto PDMS substrates. A droplet of cells is dragged across a PDMS surface containing holes engineered to trap individual cells. We demonstrate this can be achieved with the spherical bacterium Staphylococcus aureus: the cells are deposited, imaged and growth re-established on the substrate. The range of potential applications for this technique will be discussed, including population-wide response to antibiotic treatment, communication mechanisms between members of a community, and fabrication of micro-robots and active matter systems.

[1] M.E. Lidstrom, et al., Nat. Chem. Biol. 6, (2010).
[2] A. Dragoš, et al., Curr. Biol. 28, (2018).
[3] K. Lewis, Nat. Rev. Microbiol. 5, no. 1 (2007).
[4] S. Ni, et al., Sci. Adv. 2, (2016).

Particle Laden Porcine Gastric Mucin Strength

Caroline E. Giacomin[1], Peter Fischer[1]
[1] Food Process Engineering, D-HEST, ETH Zurich

In humans, mucus can be found in the respiratory, gastrointestinal, and vaginal tracts. It forms the final barrier for the epithelium which transfers particles into the body. The structure of mucus is primarily composed of mucin, a glycosylated protein with negative charge. Mucus also contains water, proteins, lipids, salts, and cellular debris [1]. These components affect mucus behavior and are dependent on surrounding composition. Mucins form a mesh-like structure and conveyance of particles is limited by the mesh pore size and viscoelasticity of the network [2]. Depending on the surrounding environment, mucus preferentially absorbs different sized particles. Polymer particles (polyethylene glycol coated carboxylated polystyrene) with 100 nm diameters were immobilized by cervicovaginal mucus while 500 nm diameters were able to penetrate [3]. In contrast, for respiratory mucus they found immobilization of 500 nm particles and 40 % mobility of 100 nm diameters. In the gastrointestinal tract 100 nm particles were uninhibited by mucus and 500 nm particles were slightly inhibited [4]. Thus, mucus presents different pore sizes in cervicovaginal, gastrointestinal, and respiratory environments [3]. The ability of microbes, drugs, nutrients, pollutants, or other particles to reach the epithelium through a mucus layer is dependent on their ability to be conveyed by said mucus layer [1]. While some penetrating particles are beneficial to the body, others cause disease or breakup of mucus. Herein we analyze particles effect on mucus structure breakup; both introduced during formation and added post-formation. Particle size, type, and charges are varied, and bulk shear rheology is used to analyze the structure strength.

[1] J.Y. Lock, et al., Adv. Drug Deliv. Rev. 124, 34 (2018).
[2] S.K. Lai, et al., Proc. Natl. Acad. Sci. U.S.A. 104, 1482 (2007).
[3] B.S. Schuster, et al., Biomaterials 34, 3439 (2013).
[4] B.H. Bajka, et al., Colloids Surf. B 135, 73 (2015).

A Biomimetic Macroporous Hybrid Scaffold with Sustained Drug Delivery for Enhanced Bone Regeneration

Seunghun S. Lee[1], Matthias Santschi[1], Stephen J. Ferguson [1]
[1] Orthopaedic Technology, D-HEST, ETH Zurich

Bone regeneration is a complicated physiological process regulated by several factors. In particular, a bone-mimicking extracellular matrix and available osteogenic growth factors such as bone morphogenetic protein (BMP) have been regarded as key factors to induce bone regeneration. In this study, we developed a biomimetic hybrid scaffold (CEGH) with sustained release of BMP-2 that would result in enhanced bone formation. This hybrid scaffold composed of BMP-2 loaded cryoelectrospun poly ε-caprolactone (PCL) (CE) surrounded by macroporous gelatin/heparin cryogel (GH), is designed to overcome the drawbacks of relatively weak mechanical properties of cryogel and poor biocompatibility and hydrophobicity of electrospun PCL. The GH component of the hybrid scaffold provides a hydrophilic surface to improve the biological response of the cells while the CE component increases the mechanical strength of the scaffold, to provide enhanced mechanical support for the defect area and a stable environment for osteogenic differentiation. After analysing characteristics of the hybrid scaffold such as hydrophilicity, pore difference, mechanical properties and surface charge, we confirmed that the hybrid scaffold group shows enhanced cell proliferation rate and apatite formation in simulated body fluid. Then, we evaluated drug release kinetics of CEGH and confirmed the sustained release of BMP-2. Finally, the enhanced osteogenic differentiation of CEGH with sustained release of BMP-2 was confirmed by Alizarin Red S staining, and real-time PCR analysis.

This project has received funding from the European Union's Horizon 2020 research and innovation programme under the Marie Skłodowska-Curie grant agreement No 812765.

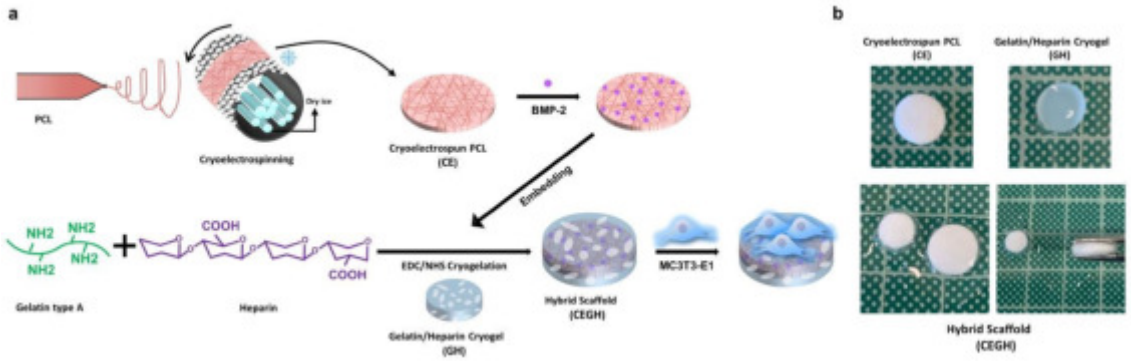

Fig.: Fabrication of hybrid scaffold (CEGH) (a) Schematic illustration of Hybrid Scaffold (CEGH). First, cryoelectrospun fiber (CE) was fabricated with PCL via cryoelectrospinning. Then, after loading BMP-2, CE is coated with GH, which was synthesized from crosslinking between gelatin and heparin by EDC/NHS mediated cryogelation process, and the CEGH is fabricated as a result. (b) Representative photographs of CE (top left), GH (top right) and CEGH (bottom). The images of CEGH show various size of CEGH based on the size of CE (left CEGH: Ø6mm and right CEGH: Ø8mm).

Hybrid Magnetoelectric Microrobots for Biomedical Applications

Xiang-Zhong Chen[1], Fajer Mushtaq[1,2], Harun Torlakcik[1], Anastasia Terzopoulou[1,3], Donghoon Kim[1], Xiaopu Wang[2], Josep Puigmartí Luis[3], Bradley J. Nelson[2], Salvador Pané[1]
[1] Materials for Robotics, D-MAVT, ETH Zurich
[2] Multi-Scale Robotics, D-MAVT, ETH Zurich
[3] Biochemical Engineering, D-CHAB, ETH Zurich

Microrobots are emerging candidates for targeted delivery of therapeutic interventions. The advantage of these microdevices over other small-scale therapeutic delivery systems is their controlled locomotion and thus accurate targeting ability. Magnetoelectric materials, which can convert magnetic input into electric output, can provide microrobotic devices not only the feasibility of being maneuvered with non-invasive magnetic fields, but also more functionalities as they can wirelessly generate electric charges. For example, the electric charges endowed microrobots the ability of inducing electrochemical reactions, which is noteworthy because more than 80 percent of vital biochemical reactions in cells are redox reactions. In this presentation, we will present different microrobots with magnetoelectric properties for targeted therapeutics. Devices with various architectures such as artificial bacteria flagella and core-shell nanowires will be shown. Materials ranging from metals and ceramics to polymeric materials are selected and combined with different fabrication techniques (e.g. template-assisted electrodeposition, sol-gel coating, photolithography, physical vapor deposition). Magnetic manipulation is employed to actuate these microrobots in aqueous environments that mimic different body fluids. We demonstrate that these magnetoelctric microrobots with distinct magnetic stimuli resulting from the same energy source – rotating magnetic fields for steering and alternating magnetic fields for functionality triggering – have the ability to either deliver drugs effectively to the targeted site while minimizing side effects of drugs administered systemically, or deliver cells and induce their differentiation in-situ for tissue regenerative purpose.
[1] X.-Z. Chen, et al., Mater. Horiz., 3, 113 (2016).
[2] M. Hoop, et al., Sci. Rep., 7, 4028 (2017).
[3] X.-Z. Chen, et al., Adv. Mater., 29, 1605458 (2017).
[4] X.-Z. Chen, et al., Adv. Mater., 30, 1705061 (2018).
[5] X.-Z. Chen, et al., Mater. Horiz., 6, 1512 (2019).
[6] M. Dong, et al., Adv. Funct. Mater., 30, 1910323 (2020).

Biomaterial Design & Characterization

Why Does Freezing Cause so Much Damage?

Dominic Gerber[1], Robert W. Style[1]
[1] Soft & Living Materials, D-MATL, ETH Zurich

It is well known that when water freezes it can generate large pressures and be very destructive. Although this is commonly attributed to the expansion of water during freezing, experiments suggests that this actually plays only a minor role. Indeed, porous materials soaked in benzene (which contracts upon freezing) show similar levels of damage to the same, water-soaked materials upon freezing. We study the forces around growing ice crystals to better understand freezing-induced damage. We measure the involved forces with Tracion Force Microscopy (TFM), where the forces exerted by the ice on a well-characterised elastic substrate are precisely measured with confocal microscopy. Surprisingly, we were able to measure surprisingly large pressures around ice crystals in an open water channel. The pressure is also extremely localised, which leads to a large propensity for causing damage. We connect this to the ice-crystal microstructure, and the process of cryosuction.

Addressable Microfluidic Platform for Cultivation and Monitoring of Individual Microbial Cells

Petra Juskova[1], Lucas Armbrecht[1], Steven Schmitt[2], Martin Held[2], Petra S. Dittrich[1]
[1] Bioanalytics, D-BSSE, ETH Zurich
[2] Bioprocess Laboratory, D-BSSE, ETH Zurich

Rapid Prototyping and Multiplexed Surface Functionalization of Thermoplastic Lab-on-chip Devices

André Kling[1], Petra S. Dittrich[1]
[1] Bioanalytics, D-BSSE, ETH Zurich

DNA Aptamer-functionalized Quartz Nanopipettes for Serotonin Sensing from Neurons

Nako Nakatsuka[1], Alix Faillétaz[1], Krishna C. Vadodaria[2], Dominic Eggemann[1], Fred H. Gage[2], János Vörös[1], Dmitry Momotenko[1]
[1] Biosensors & Bioelectronics, D-ITET, ETH Zurich
[2] Laboratory of Genetics, Salk Institute for Biological Studies, La Jolla

Advancing our understanding of neuronal communication necessitates biochemical sensors that approach the spatial resolution of chemical signalling via neurotransmitters at synapses that span only ca. 20 nm across. We have developed artificial nanopores in the form of quartz nanopipettes with 10 nm orifices functionalized with molecular recognition elements termed aptamers. Aptamers are systematically designed oligonucleotide receptors that exhibit highly specific and selective recognition of targets such as serotonin [1]. Nanoscale confinement of ion fluxes, analyte-specific changes in molecular conformation of aptamer species, and related surface charge variations enable specific and selective serotonin sensing. We demonstrated the capacity to detect physiologically relevant differences in serotonin amounts in complex media collected from human induced pluripotent stem cell-derived serotonergic neuron cultures [2]. Human serotonergic neurons treated with the antidepressant and selective serotonin reuptake inhibitor, Citalopram, or exposed to KCl that triggers neuronal depolarization, exhibited higher serotonin release into the extracellular media. By interrogating the sensing mechanism and validating detection in clinically relevant samples, we demonstrate the potential of conformationally changing aptamer-modified nanopipettes as a rapid, label-free, and translatable nanotool for diverse biological systems.

[1] N. Nakatsuka, et. al., Science 362, 319 (2018).
[2] K.C. Vadodaria, et. al., Mol. Psychiatry, 24, 808 (2019).

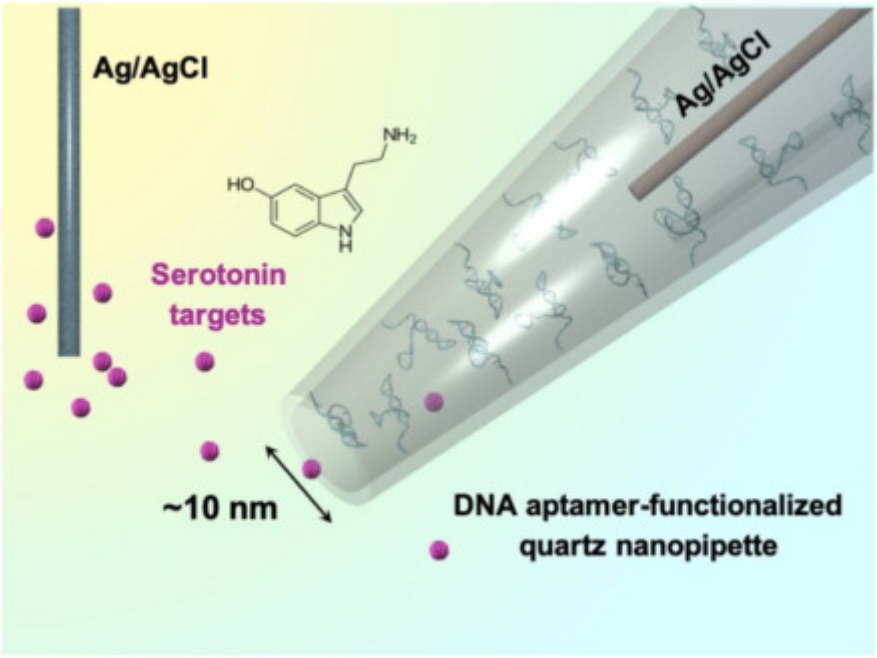

Fig.: Schematic of DNA aptamer-functionalized quartz nanopipettes. The current is measured between two Ag/AgCl quasi-reference counter electrodes, one inside the nanopipette and the other in the bulk solution. Flux of serotonin targets through the ~10 nm opening of the nanopipette is transduced as a change in current response due to aptamer conformational rearrangement upon target recognition, which alters the ionic permeability inside the nanopipette.

Towards the Fluorescent Investigation of Spatiotemporal Membrane Tension Changes in Biological Membranes During Micromanipulation

Ines Lüchtefeld[1], Christoph Gäbelein[2], Janos Vörös[1], Massimo Vassalli[3], Tomaso Zambelli[1]
[1] Biosensors & Bioelectronics, D-ITET, ETH Zurich
[2] Institute of Microbiology, D-BIOL, ETH Zurich
[3] James Watt School of Engineering, University of Glasgow

AFM Integrated Nanopores for Single-Cell Secretomics

Tilman Schlotter[1], Sean Weaver[1], Csaba Forró[1,2], Dmitry Momotenko[1], János Vörös[1], Tomaso Zambelli[1], Morteza Aramesh[1,3]
[1] Biosensors & Bioelectronics, D-ITET, ETH Zurich
[2] Department of Chemistry, Stanford University
[3] Applied Mechanobiology, D-HEST, ETH Zurich

Ions and biomolecules secreted from single cells are the key signalling factors to enable the study of cell-cell interactions as well as the interaction of cells with the extracellular matrix. Any dysfunction of these trafficking routes causes severe problems that lead to a variety of diseases, such as cancer and autoimmunity [1]. Striving for more sensitive and selective single-molecule sensing techniques, nanopore devices have emerged as a promising and intriguing technology [2]. However, on-demand pore size adjustability, durability and the limitation in nanopore engineering remain bottlenecks for practical applications of single-molecule sensing, such as secretomics and proteomics. In order to overcome those challenges, we introduce an AFM integrated nanopores sensor. The measurement of single-molecules next to mouse embryonic fibroblasts allows for live-detection of fibronectin (220 kDa) protein secretion. The time-resolved secretion from neurons over several hours furthermore demonstrates the unique capability to investigate the evolutionary life of single-cells. This provides a tool for biological disciplines that enables studying developmental biology, secretome-based communication such as in neural/immunological synapses, as well as monitoring antibody secretion from immune system cells for drug screening/discovery.

[1] W.A. Catterall, et al., Neuron 26, 13 (2000).
[2] L. Restrepo-Pérez, et al., Nat. Nanotechnol. 13, 786 (2018).

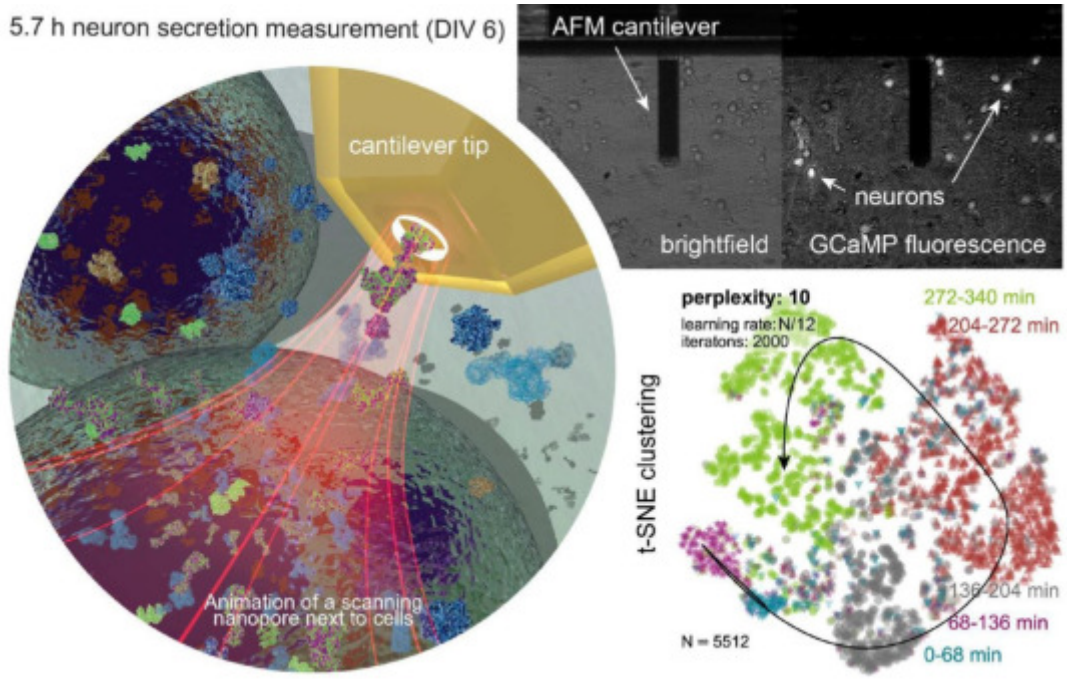

Fig.: Evolutionary single-neuron secretion visualized with t-SNE clustering using a force-controlled nanopore.

In-droplet Electrophoretic Separations using Carbon-based Electrodes

Mario A. Saucedo-Espinosa[1], Petra S. Dittrich[1]
[1] Bioanalytics, D-BSSE, ETH Zurich

In this work, an electrophoretic separation is induced inside droplets as they move through a microfluidic channel. An electric field is generated using two liquid electrodes that run parallel to the channel sidewalls. Thin PDMS membranes (100 µm) doped with carbon nanotubes enable electrical currents inside droplets. After droplet generation, all analytes are uniformly distributed in the whole droplet volume. As droplets move between the parallel electrodes, negatively-charged analytes migrate towards the top-half of droplets until the bottom-half is analytes-depleted. Droplets are then split in two: one containing the (negatively-charged) enriched analytes and one containing purified buffer. In order to test the performance of our system, fluorescently-labelled biomolecules with different sizes were enriched: nucleic acids, peptides and proteins. The fluorescence intensity of droplets was recorded to determine the enrichment performance of the system at several electric potentials, droplet velocities, and ionic strengths. The results that are presented demonstrate the potential of our system for the manipulation of small analytes in throughputs as high as 10 droplets per second. We believe the method can be integrated in various biochemical workflows performed in droplets in the future [1].

[1] X. Niuet, et al., Anal. Chem. 85, 8654 (2013).

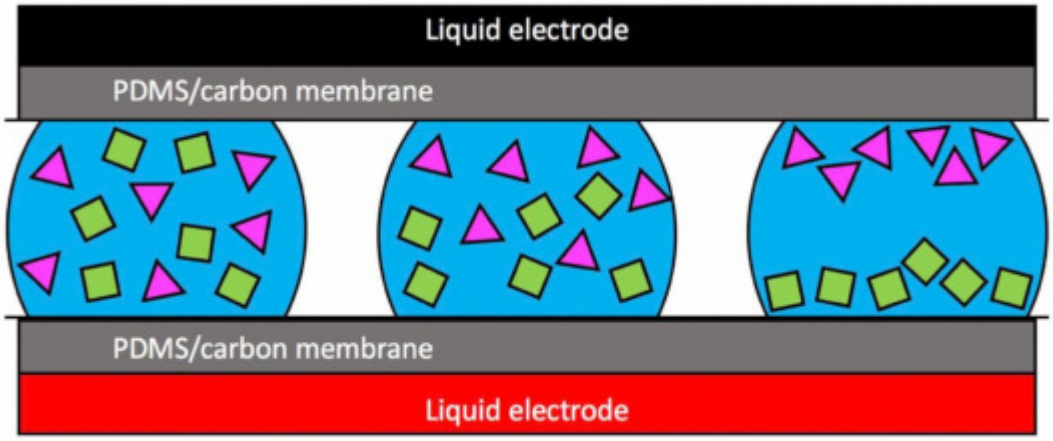

Fig.: Schematic concept of the in-droplet electrophoretic system. As the droplet moves (from left to right), the electric field established by the carbon nanotube-based electrodes transport charged molecules within the droplets to one side, depending on the surface charge of the molecules.

Transparent Nacre-inspired Composite Materials

Tommaso Magrini[1], Madeleine Fellner[2], Alessandro Lauria[2], Simon Moser[1], Florian Bouville[3], André R. Studart[1]
[1] Complex Materials, D-MATL, ETH Zurich
[2] Multifunctional Materials, D-MATL, ETH Zurich
[3] Centre for Advanced Structural Ceramics, Department of Materials, Imperial College London

Nacre is a biological material, which exhibits remarkable fracture resistance, despite being constituted up to 95% by brittle components. This property arises from its brick-and-mortar microstructure that has been a source of inspiration for the synthesis of strong and tough materials. By fabricating nacre-like porous glass scaffolds and infiltrating them with a refractive index matching polymer, the structure of nacre can be mimicked, while also rendering an optically clear composite [1]. Transparent nacre-like composites exhibit high transmission haze. A significant portion of the transmitted light is affected by scattering phenomena and is quantified by comparing inline transmittance with total diffuse transmittance (Fig.). Haze in transparent nacre-like composites is caused by imperfect refractive index matching between the organic matrix and the glass scaffold across the visible range, as well as by the defects in the composite microstructure. By characterizing the haze, and understanding its origin, the transparency of the composites can be further improved. The tradeoff between sets of antagonistic properties such as strength and toughness as well as toughness and transparency, makes transparent nacre-like composites a promising new material class which can compete with traditional glasses for technological applications such as phone screens and protective retro-illuminated displays.

[1] T. Magrini, et. al., Nat. Commun. 10, 2794 (2019).

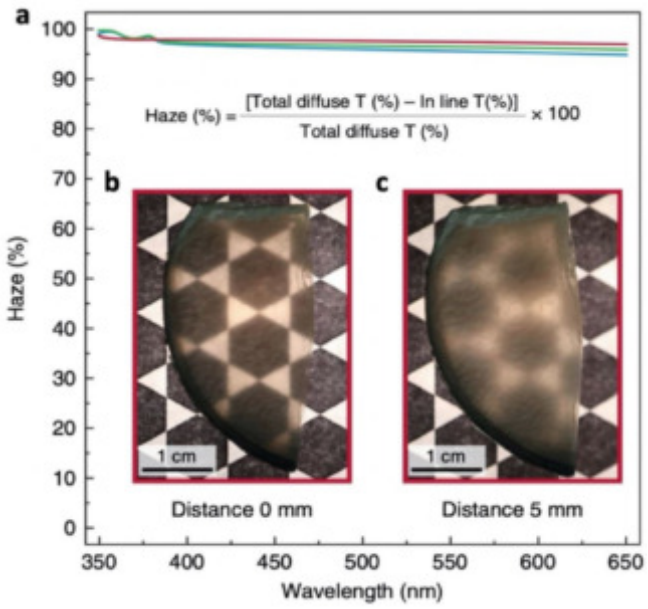

Fig.: (a) Haze, the ratio between diffuse transmittance divided by total diffuse transmittance, (b) composite on retro-illuminated pattern and (c) composite 5 mm above illuminated surface [1].

High Voltage Insulators Based on Pultruded Thermoplastic Composite Cores

Maximilian Volk[1], Shelly Arreguin[1], Joanna Wong[2], Christiane Bär[3], Frank Schmuck[3], Paolo Ermanni[1]
[1] Composite Materials & Adaptive Structures, D-MAVT, ETH Zurich
[2] Mechanical & Manufacturing Engineering, University of Calgary
[3] Pfisterer Switzerland AG, Malters

High voltage insulator rods are key components in operational safety and efficiency in the transmission of electrical power [1]. With increasing worldwide energy demand, it is necessary to implement manufacturing routes to accommodate larger diameter insulator cross sections. Current strategies use thermoset pultrusion based processing with glass fibres and epoxy resin. However, due to potential defects caused by its exothermic polymerisation behaviour [2] new methodologies must be developed. In this study, a novel pultrusion concept has been developed at CMASLab in cooperation with Pfisterer Switzerland AG, investigating the suitability of different thermoplastic/ glass-fibre composites through a combination of insulator specific mechanical, chemical and electrical tests. The process is represented in the figure below and consists of melting the commingled thermoplastic and glass fibres in a circular, tapered die to impregnate the material and then cool the composite rod until solidification. The results show that temperature, pulling speed as well as throughput are the primary parameters influencing the quality of the material. The insulator specific tests revealed different types of porosity influencing the electrical breakdown behaviour, chemical degradation of the fibre-matrix interface as well as different resistances to thermal degradation. Overall, polyethyleneterephthalate (PET) successfully passed all tests and constitutes the most promising candidate for high voltage insulator applications.

[1] K.O. Papailiou, et al., Power Syst. 75, (2013).
[2] T.A. Bogetti, J. Compos. Mater. 26, 626, (1992).

Energy, Electronics & Devices

Lithium Ion Battery Separators: The Influence of Separator Structure on Battery Performance

Christina Sauter[1], Raphael Zahn[1], Vanessa Wood[1]
[1] Material & Device Engineering Group, D-ITET, ETH Zurich

Separators in Lithium Ion Batteries (LIBs) are electronically isolating membranes that prevent physical contact between the two electrodes while allowing ionic transport. Therefore, they are considered to be a crucial part in battery safety [1]. Our research group developed an approach to visualize and quantify LIB separators with focused ion beam scanning electron microscopy (FIB-SEM) [2]. These 3D reconstructions of commercially available separators allow us to calculate the effective transport coefficient (ratio between porosity and tortuosity), which is used to characterize LIB separator performance and compare it with experimentally measured values. Here, we apply concepts from the theory of partial wetting to explain the amount of gas entrapment that occurs during electrolyte infilling and show that this can explain the lower than expected effective transport coefficients that are measured experimentally. Quasi-static infilling simulations on 3D reconstructions of the separator structure indicate that there can be up to 30% gas entrapment upon infilling due to the geometry of the separator, which results in a reduction of effective transport by >40%. This work highlights the importance of optimizing not only the physio-chemical properties of the electrolyte and pore surfaces, but also the 3D structure of the pore space which has a direct influence on battery performance as incomplete filling negatively impacts electrochemical performance, cycle life, and safety of cells [3].

[1] S.S. Zhang, J. Power Sources 164, 351 (2007).
[2] M.F. Lagadec, et al., Electrochem. Soc. 163, 992 (2016).
[3] C. Sauter, et al., J. Electrochem. Soc., submitted (2020).

Comparative Studies on $LiNi_{0.5}Mn_{0.5-x}Co_xO_2$ Cathode Materials

Rajalakshmi Senthil Arumugam[1], Ramesh Shunmugasundaram[1], Vanessa Wood[1]
[1] Materials & Device Engineering, D-ITET, ETH Zurich

Magnetic Alignment of Nanowires for Next Generation Stretchable Electronics

Byron Llerena Zambrano[1], Csaba Forró[1], Erik Poloni[2], Aline Renz[1], Qiang Zhang[3], Robert Hennig[1], André R. Studart[2], William R. Taylor[3], János Vörös[1]
[1] Bioelectronics & Biosensors, D-ITET, ETH Zurich
[2] Complex Materials, D-MATL, ETH Zurich
[3] Movement Biomechanics, D-HEST, ETH Zurich

Stretchable electronics has attracted scientific interest during the last few years. By embedding conductive nanowires, randomly assembled, into an elastomeric matrix, a percolated conductive network is created. Once embedded, the composite is granted with conductivity even under large deformations. Although this approach has proven valid, control over the electrical properties is poor due to the lack of control over the structure of the network. Here we report a simple and scalable technique to assemble and transfer high-density ordered structures of nanowires. First, manipulation of nanowires in a solution is possible by coating them with small amounts of Super Paramagnetic Iron Oxide Nanoparticles and applying low magnetic fields, following a method reported by Erb et al. [1]. High-density ordered assemblies were demonstrated with one of the most common deposition techniques for NWs: vacuum filtering. Scanning electron microscopy images showed the successful ordered assembly of large amounts of silver and gold nanowires. The architecture of the assembly had a large influence on the strain-dependent behaviour of the conductivity as expected from simulations. We believe the field of stretchable electronics can benefit from this technique as well as other fields such as transparent electrodes, optics.

[1] R.M. Erb, et al., Soft Matter 7, 8757 (2011).

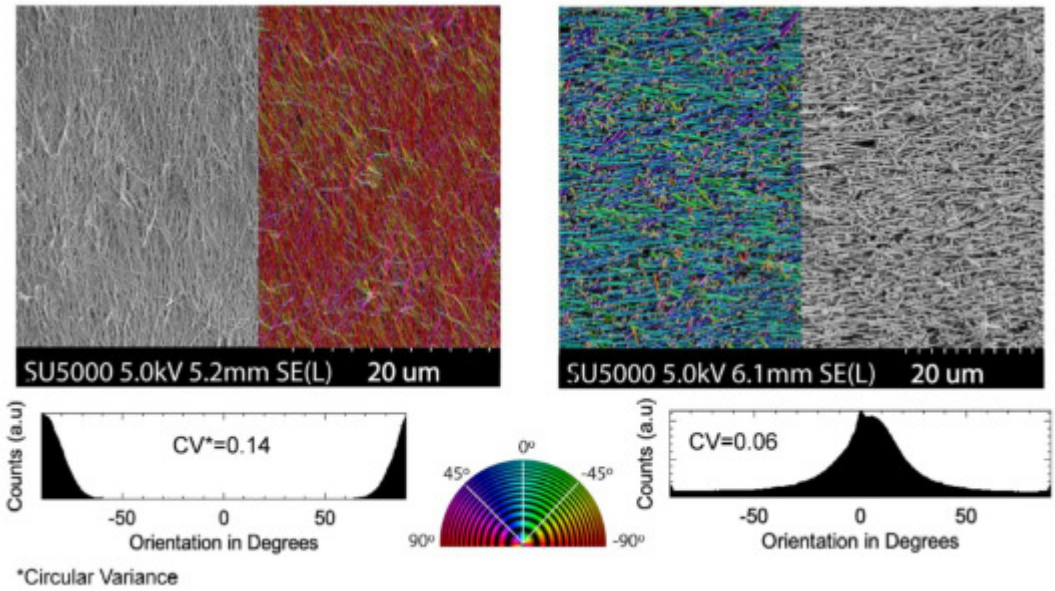

Fig.: SEM image of high-density ordered structures of: (Left) Silver nanowires and (Right) Gold nanowires. Low degree of circular variance (CV) is observed in both. Color mapping shows orientation tendency.

Inorganic Chemistry & Nanocrystal Design

Strategies for Enhancing the Photolumniescence of CdSe Magic-Sized Clusters

Andrew B. Pun[1], David J. Norris[1]
[1] Optical Materials Engineering, D-MAVT, ETH Zurich

As the field of semiconducting quantum dots (QDs) continues to mature, the variation of nanocrystal sizes present in a synthesized sample is still an obstacle. Because the properties of QDs are size dependent, it is crucial to produce QD samples of only one nanocrystal size. This will allow for accurate study of structure-property relationships. Magic-sized clusters (MSCs) circumvent the polydispersity seen in QDs, as growth is discrete and limited to only certain sized clusters. Synthesis can be optimized such that few cluster sizes are synthesized, which can then be separated to provide monodisperse QDs. In spite of this promise, MSCs remain poorly studied. MSCs typically exhibit broad emission with low photoluminescence quantum yields (PLQY). This presentation will describe our efforts towards CdSe MSCs with sharp, high efficiency PLQY. We achieved this by tuning the surface chemistry of existing clusters. These CdSe MSCs were coated with a higher band gap shelling material to provide highly luminescent core-shell MSCs. These bright, monodisperse MSCs will allow for a variety of studies on the source of their optoelectronic properties. Furthermore, these MSCs are an exciting candidate for use in a variety of applications such as lighting and lasing.

Nitrogen Doped TiO_2 Nanoparticle-based Aerogels for Visible-light-driven Photocatalytic H_2 Production

Junggou Kwon[1], Murielle Schreck[1], Markus Niederberger[1]
[1] Multifunctional Materials, D-MATL, ETH Zurich

TiO_2 nanoparticle-based aerogels, three-dimensional assemblies of crystalline TiO_2 nanoparticles, are promising photocatalysts due to their large surface area, remarkable porosity, translucency, and the nanoscale characteristics of the semiconducting building blocks. Recent studies in our group showed that metal-decorated TiO_2 nanoparticle-based aerogels are effective for gas-phase photocatalytic CO_2 reduction and H_2 production [1,2]. However, TiO_2 nanoparticle-based aerogels remain limited to UV-driven photocatalysts due to the intrinsic wide bandgap (3.2 eV). To increase the conversion efficiency from solar energy to chemical energy, visible-light sensitization of TiO_2 is necessary. In this study, we present a facile method to dope the TiO_2 nanoparticle-based aerogels postsynthetically to make them visible-light active for photocatalytic H_2 production. CVD-based gas-phase reaction and plasma utilization at low temperature provided efficient nitrogen doping to TiO_2 aerogel monoliths without affecting the initial properties. Nitrogen doping remarkably enhanced visible-light absorption and generated more than 60 times higher H_2 production compared to undoped TiO_2 aerogel under visible light. Our approach of gas-phase nitridation of preformed monolithic TiO_2 nanoparticle-based aerogels offers a powerful tool to improve their properties as visible-light active photocatalysts.

[1] F. Rechberger, et. al., Mater. Horiz. 4, 1115 (2017)
[2] A.L. Luna, et. al., Appl Catal B Environ. 267, 118660 (2020)

How Magic-Sized Clusters Grow: A Microscopic Theory

Sergio Mazzotti[1], Aniket Mule[1], and David J. Norris[1]
[1] Optical Materials Engineering, D-MACT, ETH Zurich

Magic-sized clusters (MSCs) are small semiconductor nanocrystals with well-defined structures and characteristic optoelectronic properties. Only a few “magic” sizes with superior thermodynamic stability are believed to exist. They have been shown to grow sequentially, meaning that one “magic” size transitions directly to the next. However, the origin of their stability and the mechanism that determines their growth remain puzzling. Our experiments, in line with previous reports, suggest that MSCs are tetrahedral in shape. Based on these findings, we present a microscopic model that rationalizes their stability and growth. By combining classical nucleation theory and the tetrahedral shape of MSCs, our model explains both why MSCs correspond to local minima in a free-energy landscape and why they grow sequentially. Our model can help find other crystalline materials exhibiting the same “magic” growth behavior.

Size and Composition Controlled Intermetallic Nanocrystals via Amalgamation Seeded Growth

Jasper Clarysse[1], Maksym Yarema[2], Annina Moser[1], Olesya Yarema[1], Vanessa Wood[1]
[1] Materials & Device Engineering, D-ITET, ETH Zurich
[2] Chemistry & Materials Design, D-ITET, ETH Zurich

Intermetallic nanocrystals are long-range ordered alloys, which feature combined properties of the incorporated metals and often exhibit synergistic effects. As a result, research interests in these materials is surging and they are studied for a wide-range of applications including catalysis, thermoelectrics, plasmonics, superconductor technologies, MRI contrast agents, phase-change memories and as functional materials for energy storage. Considering catalysis for example, ordered intermetallic nanocrystals are envisioned to be key materials for tackling various selectivity challenges, including the conversion of CO_2 to value-added products. Nevertheless, progress in synthesis methods towards intermetallic nanocrystals is highly desirable as only a fraction of the existing compounds have been achieved yet. We developed a wet-chemistry colloidal synthesis route towards well-defined intermetallic nanocrystals based on amalgamation seeded growth. This synthesis method is characterized by its generality as various metal nanocrystal seeds (e.g. Au, Ag, Cu, Pd, Ni) can be amalgamated with low-melting point metals (e.g. Ga, In, Zn) into intermetallic nanocrystals. Furthermore, we demonstrate excellent control over size and composition of the synthesized nanocrystals. We gained insights into the mechanistic aspects of the reaction through profound analysis and we also discovered some exceptional nanocrystal structures resulting from the synthesis, such intermetallic nanocrystals with bend lattices and voids.

[1] J. Clarysse et al. in progress.

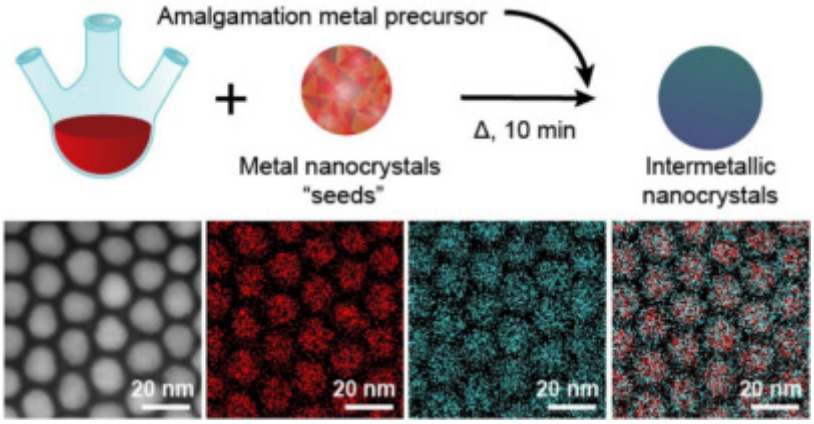

Fig.: Reaction scheme for the amalgamation seeded growth synthesis and STEM EDX maps of $AuGa_2$ nanocrystals as an example of synthesized nanocrystals [1].

Amide-Promoted Synthesis of $AgSbTe_2$ and $Ag_xSb_{1-x}Te_{1.5-x}$ Nanocrystals

Annina Moser[1], Olesya Yarema[1], Maksym Yarema[2], Vanessa Wood[1]
[1] Materials & Device Engineering, D-ITET, ETH Zurich
[2] Chemistry & Materials Design, D-ITET, ETH Zurich

Ternary tellurides have gained increasing interest as materials for thermoelectrics due to high phonon scattering while exhibiting good electrical conductivity. At the same time, there is a need for a widening of the recipe catalogue for telluride nanocrystals. We present a convenient amide-promoted synthesis to achieve ternary Ag-Sb-Te nanocrystals of small size with narrow size distributions (e.g., diameters of 3.5 ± 0.8 nm). By controlling the ratio of the cation precursors, stoichiometric $AgSbTe_2$ and $Ag_xSb_{1-x}Te_{1.5-x}$ nanocrystals (x is from 0.3 and 0.6) are achieved. We comment on the mechanism that enables this synthesis as well as the possibility for it to be further optimized and extended to other ternary tellurides [1].

[1] A. Moser, et. al., J. Mater. Chem. C, submitted.

Liquid Phases & Polymers

Thermally Superactive Nanomagnets Obtained with Interfacial Dzyaloshinskii-Moriya Interaction

Kevin Hofhuis[1,2], Aleš Hrabec[1,2,3], Hanu Arava[1,2], Naëmi Leo[1,2,4], Yen-Lin Huang[5], Rajesh V. Chopdekar[6], Sergii Parchenko[1,2,7], Armin Kleibert[7], Sabri Koraltan[8], Claas Abert[8], Christoph Vogler[8], Dieter Suess[8], Peter M. Derlet[9], Laura J. Heyderman[1,2]
[1] Mesoscopic Systems, D-MATL, ETH Zurich and PSI
[2] Multiscale Materials Experiments, PSI
[3] Magnetism & Interface Physics, D-MATL, ETH Zurich
[4] CIC nanoGUNE, Spain
[5] Materials Science & Engineering, University of California Berkeley
[6] Advanced Light Source, Lawrence Berkeley National Laboratory (LBNL)
[7] Swiss Light Source (SLS), PSI
[8] Advanced Magnetic Sensing & Materials, University of Vienna
[9] Condensed Matter Theory, PSI

Droplet Breakup of High-viscosity-ratio Emulsions with an Optimized Interaction Chamber

Laura Wiest[1], Dominik Hug[1], Erich J. Windhab[1]
[1] Food Process Engineering, D-HEST, ETH Zurich

Nanoemulsions are optically clear, highly bioavailable and stable emulsions, which have extensive applications in the chemical, pharmaceutical and food industry. In high-pressure homogenisation processes, the design of the interaction chamber plays an important role on droplet break-up, and especially the subsequent recoalescence. By adapting the interaction chamber design through OpenFoam CFD simulations, the flow profile within the chamber was optimized to equalize the droplets' residence time. Therefore, the improved design is expected to ensure all droplets experience a more homogenous emulsification, resulting in narrow, mono-modal particle size distributions. This study compares the emulsification performance of this optimized interaction chamber with a standard Y-type microfluidizer interaction chamber for a range of pressure drops, oil types and concentrations. For the same pressure drop, it is found that the optimized interaction chamber produced equal or smaller droplet sizes with narrower particle size distributions. With increasing disperse phase viscosity, the droplet breakup within the optimized interaction chamber was superior to the Y-type microfluidizer interaction chamber. This effect was even more pronounced with increasing pressure drops for the optimized chamber, while higher pressure drops had little to no effect on emulsions homogenized with the Y-type chamber. This study presents an optimized chamber design with a narrower residence time distribution that is beneficial for emulsification, especially for viscosity ratios above 100.

Tuning Molecular Fluorescence in Aggregated State via Polymerization-Mediated Charge Transfer

Suiying Ye[1], Tian Tian[2], Andrew J. Christofferson[3], Sofia Erikson[1], Jakub Jagielski[2], Zhi Luo[1], Sudhir Kumar[2], Chih-Jen Shih[2], Jean-Christophe Leroux[1], Yinyin Bao[1]
[1] Drug Formulation & Delivery, D-CHAB, ETH Zurich
[2] Interface & Surface Engineering of Nanomaterials, ETH Zurich
[3] Engineering & Health, College of Science, RMIT University Melbourne

Effect of Polymerization Components on Oxygen-Tolerant Photo-ATRP

Manon Rolland[1], Richard Whitfield[1],Daniel Messmer[1],Kostas Parkatzidis[1], Nghia P. Truong[1], Athina Anastasaki[1]
[1] Polymeric Materials, D-MATL, ETH Zurich

Photo-ATRP has recently emerged as a powerful technique that allows for oxygen-tolerant polymerizations and the preparation of polymers with low dispersity and high end-group fidelity. However, the effect of various photo-ATRP components on oxygen consumption and polymerization remains elusive. Herein, we employ an in situ oxygen probe and UV–vis spectroscopy to elucidate the effects of ligand, initiator, monomer, and solvent on oxygen consumption. We found that the choice of photo-ATRP components significantly impacts the rate at which the oxygen is consumed and can subsequently affect both the polymerization time and the dispersity of the resulting polymer. Importantly, we discovered that using the inexpensive ligand TREN results in the fastest oxygen consumption and shortest polymerization time, even though no appreciable reduction of $CuBr_2$ is observed. This work provides insight into oxygen consumption in photo-ATRP and serves as a guideline to the judicious selection of photo-ATRP components for the preparation of well-defined polymers.

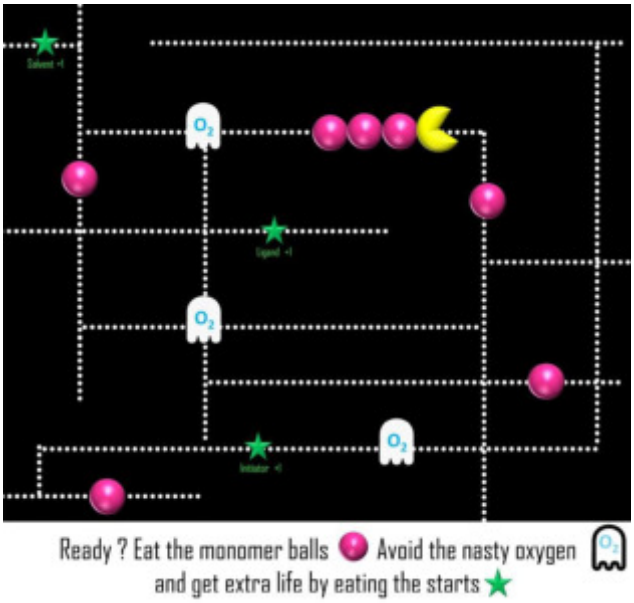

Fig.: The Pac-Man Game showing the effect of polymerization components on oxygen-tolerant photo-ATRP.

Magnetics

Magnetic Quadrupole Assemblies with Arbitrary Shapes and Magnetizations

Hongri Gu[1], Quentin Boehler[1], Daniel Ahmed[2], Bradley J. Nelson[1]

[1] Multi-Scale Robotics Lab, D-MAVT, ETH Zurich

[2] Acoustic Robotics & Systems Lab, D-MAVT, ETH Zurich

Magnetic dipole-dipole interactions govern the behavior of magnetic matter across scales from micrometer colloidal particles to centimeter magnetic soft robots. This pairwise long-range interaction creates rich emergent phenomena under both static and dynamic magnetic fields. However, magnetic dipole particles, from either ferromagnetic or paramagnetic materials, tend to form chain-like structures as low-energy configurations due to dipole symmetry. The repulsion force between two magnetic dipoles raises challenges for creating stable magnetic assemblies with complex two-dimensional (2D) shapes. In this work, we propose a magnetic quadrupole module that is able to form stable and frustration-free magnetic assemblies with arbitrary 2D shapes. The quadrupole structure changes the magnetic particle-particle interaction in terms of both symmetry and strength. Each module has a tunable dipole moment that allows the magnetization of overall assemblies to be programmed at the single module level. We provide a simple combinatorial design method to reach both arbitrary shapes and arbitrary magnetizations concurrently. Last, by combining modules with soft segments, we demonstrate programmable actuation of magnetic metamaterials that could be used in applications for soft robots and electromagnetic metasurfaces [1].

[1] H. Gu, et al., Sci. Robot. 4, (2019).

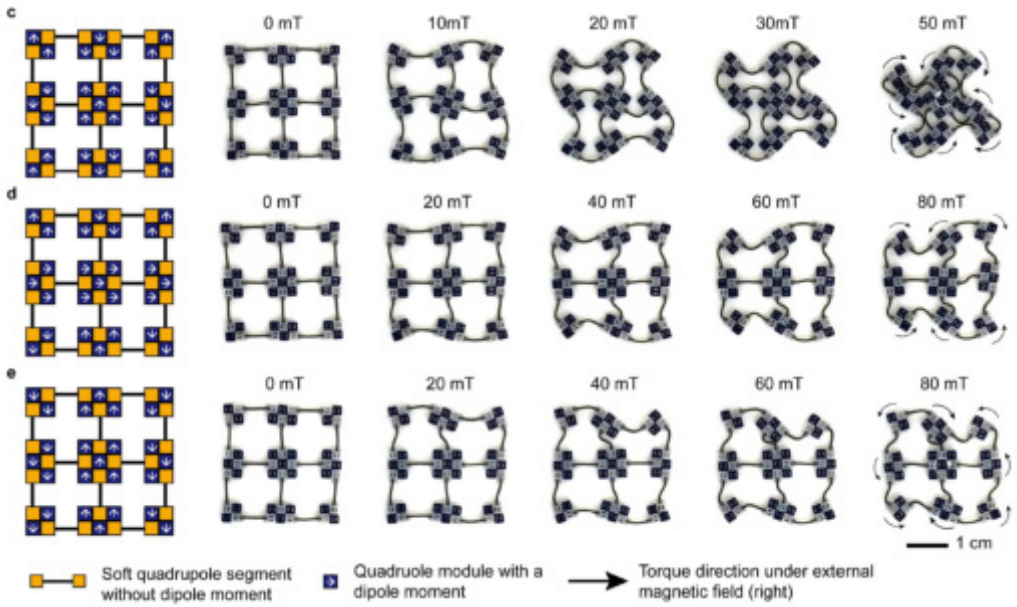

Fig.: Actuated soft structured material with programmable deformations.

Non-resonant Magnetic X-ray Diffraction to Monitor the Quenching of Anti-ferromagnetic Order of FeRh Films

Michael Grimes[1,2,3], Namrata Gurung[2,3], Dan Porter[4], Laura Heyderman[2,3], Tom Thomson[1], Valerio Scagnoli[2,3]

[1] Nano-Engineering & Spintronic Technologies, University of Manchester

[2] Mesoscopic Systems, D-MATL, ETH Zurich and PSI

[3] Multiscale Materials Experiments, PSI

[4] Diamond Light Source, Didcot

Precessional Dynamics in Antiferromagnetically Coupled Ferromagnetic Films

Jingyuan Zhou[1,2], Susmita Saha[1,2], Zhaochu Luo[1,2], Eugenie Kirk[1,2], Valerio Scagnoli[1,2], Laura J. Heyderman[1,2]
[1] Mesoscopic Systems, D-MATL, ETH Zurich and PSI
[2] Multiscale Materials Experiments, PSI

Antiferromagnetically coupled ferromagnetic films have recently attracted significant attention in magnonics due to the possibility to tune the spin-wave dispersion by altering the interlayer coupling [1], which would help to achieve spin-wave non-reciprocity. In this work, we have characterized the precessional dynamics in trilayer films with different coupling strength using the time-resolved magneto-optical Kerr effect. In addition to the acoustic and optical modes, an extra mode due to laser-induced decoupling of the ferromagnetic layers is observed [2]. Furthermore, we find that by considering the relationship between the Zeeman energy and interlayer coupling, we can separate the dynamics into three field regions, so providing an important guide for implementing antiferromagnetically coupled films in functional magnonic devices.

[1] R.A. Gallardo, et al. Phys. Rev. Appl. 12, 034012 (2019).
[2] J. Zhou, et al. submitted, (2020).

Mechanical Properties of Solids

Atomic-scale Investigations of the Invar Effect in Fe-based Bulk Metallic Glasses

Alexander Firlus[1], Mihai Stoica[1], Robin Schäublin[1], Jörg F. Löffler[1]
[1] Metal Physics & Technology, D-MATL, ETH Zurich

Magnetic bulk metallic glasses (BMGs) have a very low coefficient of thermal expansion (CTE) below the Curie temperature TC. Around TC the CTE increases abruptly by a factor of 2-10 (Fig.). This effect, known as Invar effect, is observed for all Fe-based magnetic BMGs but rarely seen in crystalline materials, with Fe-Ni being a notable exception. Explanations of the Invar effect are generally based on calculations and simulations. They rely on a crystallographic unit cell and thus have no base in amorphous materials such as BMGs.

In this work we investigate structural changes of BMGs related to the Invar effect at various length scales from the macroscopic to the atomic scale. Structural changes due to heat treatment change both the magnitude and the temperature at which the Invar effect occurs, as illustrated via X-ray diffraction (XRD) and dilatometry measurements. Furthermore, based on in-situ synchrotron XRD we will discuss how atomic arrangements (i.e. atomic distances and chemical structure) determine and influence the Invar effect in metallic systems.

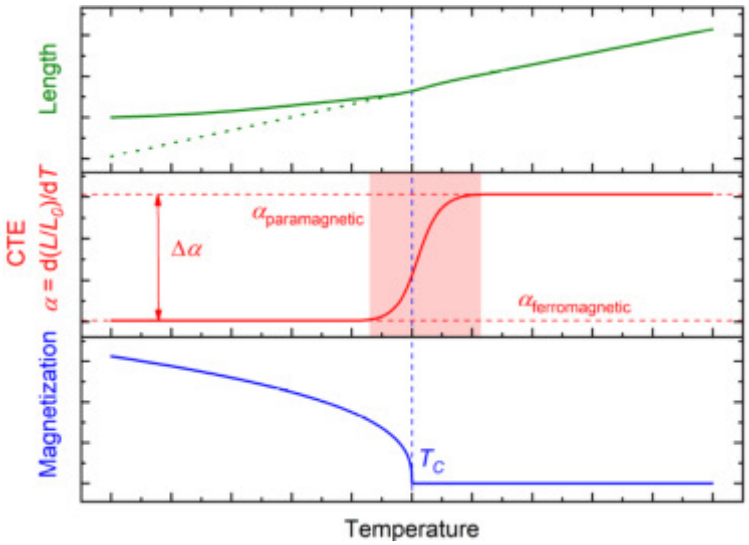

Fig.: Thermal expansion of a material revealing the Invar effect.

Ab Initio Modelling of Thermal Transport through van der Waals Materials

Sara Fiore[1], Mathieu Luisier[1]
[1] Integrated Systems Laboratory, D-ITET, ETH Zurich

We have developed an advanced modelling approach to shed light on the thermal transport properties through van der Waals materials (vdWm) made of two transition metal dichalcogenide (TMD) monolayers with partial overlap [1,2]. The latter structures could play an important role in several applications, going from next-generation transistors to ultra-scaled optical devices, provided that the heat flowing through them can be efficiently controlled. In our simulations, thermal transport is computed at the quantum mechanical level, in the ballistic limit, by combining dynamical matrices from first-principles and the Non-equilibrium Green's Function formalism. Phonons are injected into one of the TMDs and collected in the other. Since, only phonons occupying states available through the whole structure can be transmitted, the heat transferred through partially overlapping homo- or hetero-bilayers is reduced as compared to a single monolayer of one type or the other. This behaviour is observed when both different and identical TMDs form the vdWm of interest. Our work emphasizes the possibility of engineering the heat flowing through nanostructures by combining TMDs monolayers exhibiting different thermal properties.

[1] P. Ajayan, et al., Physics Today 9, 38 (2016).
[2] A.K. Geim, et al., Nature 499, 419 (2013).

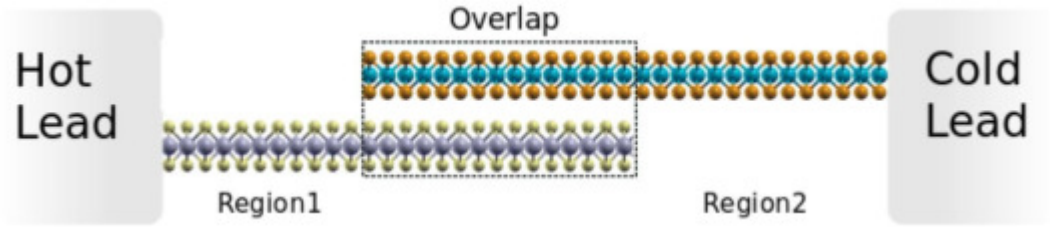

Fig.: Device simulation domain: Two TMDs monolayers with partial overlap.

Skyrmion Imaging With NV Spectroscopy and X-ray Tomography

Sam Treves[1,2,3], Valerio Scagnoli[1,3], Patrick Maletinsky[2], Laura Heyderman[1,3]
[1] Multiscale Materials Experiments, PSI
[2] Department of Physics, University of Basel
[3] Mesoscopic Systems, D-MATL, ETH Zurich and PSI

Magnetic topological structures are of scientific interest due to their potential to serve as storage and transport devices for information. One particular example is skyrmions, though much is still unknown about their formation and disappearance events, and the role that microscopic defects have in this process. Recent developments in X-ray 3D magnetic imaging, which allow for the reconstruction of 3D complex magnetic configurations [1], will allow these processes to be observed while obtaining a quantitative picture of the magnetization dynamics. This will also allow for the verification that deformed skyrmion strings elongate through a bulk sample. Simulations are currently being used to predict the behaviour of the system that should be seen when conducting nitrogen vacancy (NV) spectroscopy and X-ray 3D magnetic imaging measurements. These simulations will assist in explaining the physics behind unseen phenomena, should they occur during the experiment; for example, a change in the skyrmion state from hexagonal to elongated, due to a decrease in the exchange interaction [2].

[1] C. Donnelly, et al. Nat. Nanotechnol., (2020).
[2] V. Ukleev, et al. Phys. Rev. B. 99, 1 (2019).

Investigating Long Range Vibrations in Nanocrystal Solids

Maximilian Jansen[1], Nuri Yazdani[1], Olesya Yarema[1], Fanni Juranyi[2], Vanessa Wood[1]
[1] Materials & Device Engineering, D-ITET, ETH Zurich
[2] Neutron Scattering & Imaging, PSI

The assembly of semiconductor nanocrystals (NCs) into conductive and ordered solids is of interest for a wide range of electronic applications. Control of the constituent NCs allows for facile tuning of the NC solids electronic, structural and thermal properties. An important contributor to the thermal characteristics is the vibrational spectrum of the NC solid. We expect inter-particle vibrations, analogous to phonons on the atomic level, to be of importance for long range heat transport. These vibrational excitations involving multiple NCs are of a longer length scale than any other vibration type in the NC solid. By implementing a three-dimensional mass-spring model, we demonstrate effect of mass-spring disorder on these long-range vibrations. Further, we explore the parameter space of particle size and ligand type and their effect on the energy regime of the inter-particle vibrations [1]. Additionally, we experimentally confirm their existence through inelastic neutron scattering and determine their characteristic energy scale and density [2]. We successfully demonstrate that the energy regime of these inter-particle excitations can be engineered by varying particle size and ligand type of the NCs.

[1] M. Jansen, et. al., APL Mat. 7, (2019).
[2] N. Yazdani, et. al., Nat. Comm. 10, (2019).

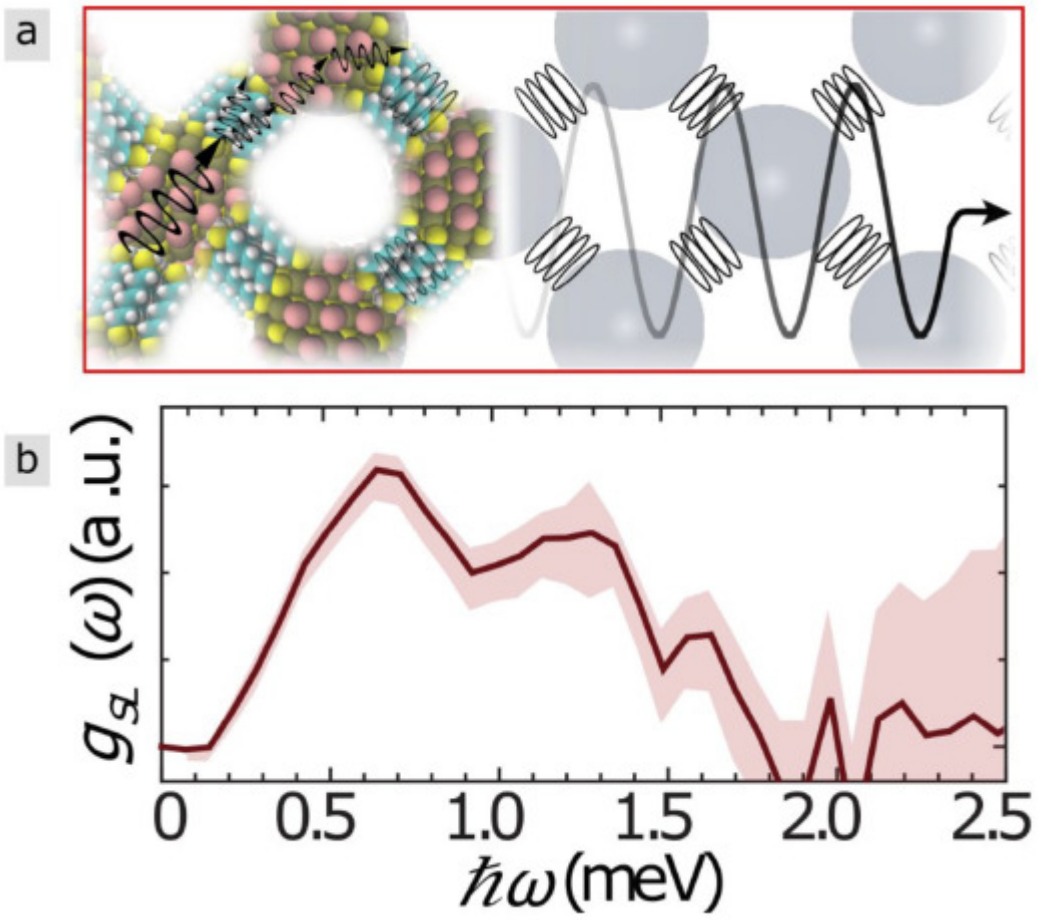

Fig.: a) Visualization of a nanocrystal superlattice and the inter-particle vibration model. b) Inter-particle vibrational density of states, measured by inelastic neutron scattering on PbS nanocrystals [2].

Probing the Limits of Strength in Diamonds: From Single- and Nano-crystalline to Diamond-like-carbon (DLC)

Ming Chen[1], Chang Liu[2], Stephan Gerstl[3], Xing Huang[3], Micha Calvo[1], Ralph Spolenak[1], Jeffrey M. Wheeler[1]

[1] Nanometalluargy, D-MATL, ETH Zurich

[2] Mechanical & Biomedical Engineering, City University of Hong Kong

[3] ScopeM, ETH Zurich

As the hardest known material, diamond represents the benchmark for the ultimate strength of materials. It is thus a very attractive material for a number of mechanical applications. Recent advances in synthesis techniques have enabled the fabrication of diamond in thin film form with various microstructures: single- and nano-crystalline and tetrahedral-amorphous or diamond-like carbon (DLC) [1,2]. Microcompression has been demonstrated to enable the interrogation of even the strongest form of diamond - a ⟨111⟩-oriented single crystal - achieving the strength limit predicted by simulations (Fig.) [3,4]. Nowadays, these allotropes of carbon with high strength and low friction are used in microelectronics and micro-electromechanical systems (MEMS) as structure components [5]. However, the effects of these new nanostructures on the mechanical properties of these allotropes is mostly unknown especially at different service temperatures. In this study, the mechanical properties of single crystalline, nanocrystalline, and amorphous forms of diamond are systematically studied by conducting in situ microcompression at various temperatures in scanning electron microscope (SEM). This allows the investigation of thermally-activated defect behavior and activation energy for several different nanostructures of diamond. This is then correlated with the deformed structures using high resolution transmission electron microscope (HRTEM) and Raman spectroscopy to interpret the deformation mechanisms.

[1] O.A. Williams, et. al., Diamond and Related Materials 20, 621 (2011).

[2] C. Liu, et. al., Carbon 122, 276 (2017).

[3] J.M. Wheeler, et. al., Nano Lett 16, 812 (2016).

[4] D. Roundy, et. al., Phys Rev B 64, (2001).

[5] L. Sekaric, et. al., App Phys Lett 81, 4455 (2002).

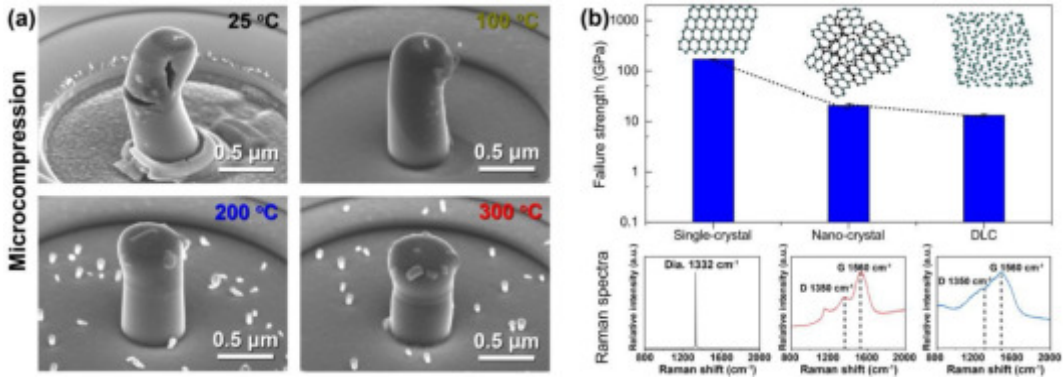

Fig.: (a) Pillar after micro-compression tests at various temperature. (b) Failure strength of single-, nano-crystalline diamonds and DLC nanopillars with 0.5 μm diameter and also the corresponding Raman spectra.

Optics, Photonics & Plasmonics

Two-Colour Diffraction Imaging of Helium Nanodroplets

Linos Hecht[1], Bruno Langbehn[2], Carlo Callegari[3], Alessandro Colombo[1], Alessandro d'Elia[3], Michele di Fraia[3], Luca Giannessi[3], Katharina Kolatzki[1], Björn Kruse[4], Ricardo Mincigrucci[3], Yevheniy Ovcharenko[6], Christian Peltz[4], Paolo Piseri[5], Oksana Plekan[3], Kevin Prince[3], Mario Sauppe[1], Björn Senfftleben[7], Saida Walz[2], Thomas Fennel[1,4], Thomas Möller[2], Daniela Rupp[1]

[1] Nanostructures & Ultrafast X-Ray Science, D-PHYS, ETH Zurich
[2] Optics & Atomic Physics, Technische Universität Berlin
[3] Elettra Sincrotrone Trieste
[4] Institut für Physik, Universität Rostock
[5] Department of Physics, Universita degli Studi di Milano
[6] European XFEL, Schenefeld
[7] Nichtlineare Optik & Kurzzeitspektroskopie, Max-Born-Institut Berlin

The structure and dynamics of short-lived and fragile nanostructures such as helium nanodroplets can be studied by diffraction imaging with the intense femtosecond pulses from short-wavelength free-electron lasers (FEL). In a single shot, a diffraction pattern of a single nanodroplet can be recorded in which the droplet's structure is encoded. Via pump-probe schemes also ultrafast structural and even electronic changes within the nanodroplet can be followed. Helium nanodroplets are produced by a cryogenic pulsed jet with sizes of several hundred nanometres. Novel two-colour capabilities at the extreme ultraviolet free-electron laser (XUV-FEL) FERMI allow for a new time-resolved imaging approach. When the nanodroplet is hit by the two-colour XUV beam, two individual diffraction images are created which can be separated by wavelength sensitive filters in front of the detector. That way it becomes possible to image the initial and an evolved state of the droplet separately. The experimental setup and the results from the proof of principle experiment will be discussed. Changes in the structure of the diffraction pattern when one colour is tuned to the 1s2p resonance of helium indicate that it is possible to trace ultrafast excitation and plasma formation on the nanoscale with two-colour diffraction imaging.

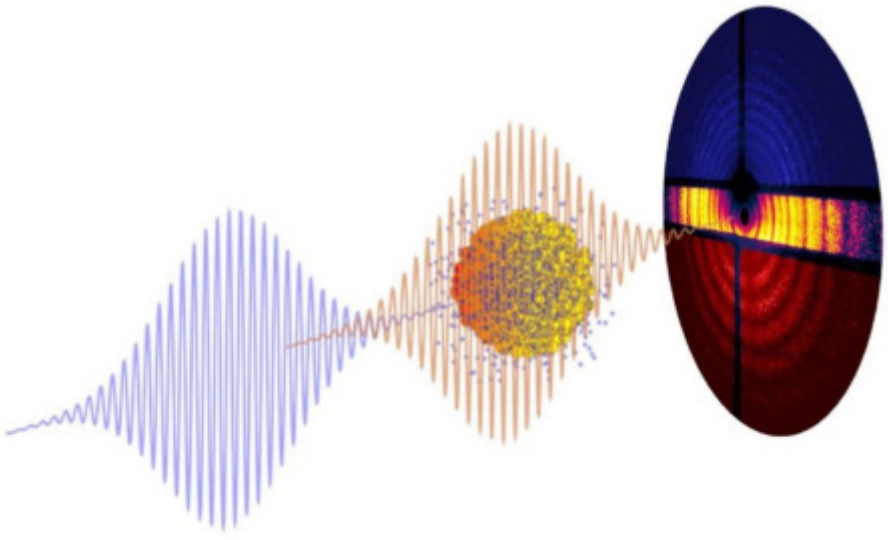

Fig.: Sketch of two-colour diffraction imaging setup.

A Local-density-of-optical-states Approach to Excited-state Dynamics of Colloidal Semiconductor Nanocrystals

Ario Cocina[1], Raphael Brechbühler[1], Maryna I. Bodnarchuck[2], Aurelio A. Rossinelli[1], Maksym V. Kovalenko[2], David J. Norris[1]
[1] Optical Materials Engineering, D-MAVT, ETH Zurich
[2] Functional Inorganic Materials, D-CHAB, ETH Zurich

Band-edge excitons of semiconductor nanocrystals feature a complex set of energy sublevels. Those sublevels affect the light-emission properties of the nanocrystals. At low temperatures, when the thermal energy of the system is comparable to the energy differences between those sublevels, multi-exponential decay dynamics of the fluorescent emission is probed with time-resolved measurements [1]. Often temperature-dependent decay studies are used to gain insight into the transition rates between sublevel states, recombination rates, and energetic ordering of the sublevels. However, such studies can sometimes yield multiple interpretations on the dynamics of the band-edge exciton. Here we show that control of the local density of optical states (LDOS) of the nanocrystal environment is another technique to probe exciton fine-structure states. As initially shown by Drexhage on europium complexes [2], the LDOS modifies the rate of radiative transitions according to Fermi's golden rule. This is experimentally achieved by placing the nanocrystals at different distances from a reflecting surface, therefore exposing them to a different LDOS. We record low-temperature time-resolved photoluminescence, which reflects changes in radiative decay rates. Using CdSe and perovskite nanocrystals, we show that our method provides a complementary tool to investigate the dynamics between excited-state energy sublevels and to estimate the quantum efficiency of the energy sublevels in the low-temperature regime. Our approach is also easily extended to other fluorescent colloidal nanocrystals.

[1] M. Nirmal, et al. Phys. Rev. Lett. 75, 3728 (1995).
[2] K.H. Drexhage, J. Lumin. 1-2, 693 (1970).

Disordered Assemblies of $LiNbO_3$ Nanoparticles for SHG in Multiple Scattering Regime

Andrea Morandi[1], Romolo Savo[1], Jolanda Muller[1], Simeon Reichen[1], Rachel Grange[1]
[1] Optical Nanomaterials, D-PHYS, ETH Zurich

Light-matter interaction in disordered and multiple scattering systems can lead to unexpected and peculiar phenomena [1]. Linear and nonlinear properties of lithium niobate ($LiNbO_3$) nanoparticles, assembled with bottom-up fabrication techniques, offer a valuable platform to investigate the transport and the generation of light in random media. In this work, we used $LiNbO_3$ cubic nanoparticles [2] to fabricate disordered and optically scattering microspheres of diameters between 2 μm and 40 μm by emulsion-driven assembly. We show that the microspheres emit second harmonic through random quasi phase matching (RQPM) [3]. The nonlinear generation is broadband and scales linearly with the volume, even for sizes of the assemblies bigger than the coherence length of the material. To quantify their scattering strength, we assembled the same nano-cubes into slabs of controlled thickness and measured the transport mean free path from total transmission measurement with an integrating sphere. Thanks to this, we show that the multiple scattering of light in the spheres is not detrimental for the broadband frequency conversion of RQPM. Our work gives evidence of RQPM for nanostructured media on a length-scale of few microns in the multiple scattering regime and propose $LiNbO_3$ assemblies as a toolbox to investigate complex and nonlinear photonics.

[1] D. Wiersma, Nat. Photon. 7, 188 (2013).
[2] F. Timpu F. et al., ACS Photonics 6, 545 (2019).
[3] M. Baudrier-Raybaut, Nature 432, 374 (2004).

Setup and Characterization of a Helium Liquid Jet for Diffraction Experiments

Katharina Kolatzki[1,2], Rico Mayro P. Tanyag[2], Georg Noffz[2], Anatoli Ulmer[2], Thomas Möller[2], Daniela Rupp[1,3]
[1] Nanostructures & Ultrafast X-Ray Science, D-PHYS, ETH Zurich
[2] IOAP, TU Berlin
[3] Ultrafast Dynamics in Nanoplasma, Max-Born-Institut Berlin

With intense XUV and X-Ray pulses from free-electron lasers (FEL) and high-harmonic generation (HHG) sources, coherent diffractive imaging of isolated nanoparticles in free flight has become possible. This allows for in-situ structure determination of fragile specimen and for time-resolved laser-matter interaction studies. In the latter case, atomic clusters are often used as targets, since they can serve as ideal model systems. However, in particular for dynamic studies, it is desirable that these targets are constant in size and spacing. Large helium droplets produced via Rayleigh-type breakup of a liquid jet meet these requirements: Compared to other types of clusters or droplets, they can exhibit very narrow size distributions and even spacing. Helium droplets also have a simple electronic structure, show interesting properties like superfluidity and can be used as a cooling matrix for embedded atoms and molecules. Recently, we have constructed and characterized a source for a helium liquid jet and subsequent droplets, which is now available for user experiments at the European XFEL's SQS endstation. Via shadowgraphy methods, we have analyzed the jet's shape and the droplet size distributions. Results from these measurements and an improved setup currently under construction at ETH will be presented.

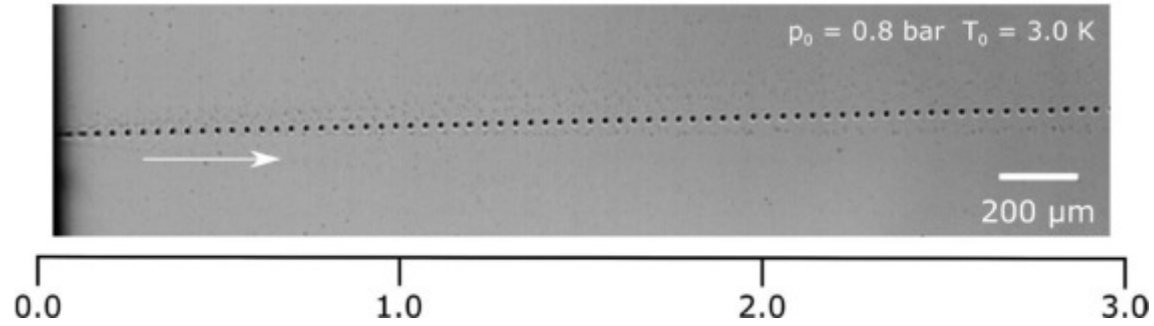

Fig.: Shadowgraphy image of a liquid helium jet, which breaks up into equidistant, uniform droplets via the Rayleigh mechanism.

Revisiting Design Principles of 2D Metallic Lasers: Coexistence and Competition of Plasmonic and Photonic Modes

Marianne Aellen[1], Aurelio A. Rossinelli[1], Robert C. Keitel[1], Raphael Brechbühler[1], Felipe V. Antolinez[1], Jian Cui[1], David J. Norris[1]
[1] Optical Materials Engineering, D-MAVT, ETH Zurich

Photoluminescence Excitation Spectroscopy on Individual Quantum Emitters

Robert C. Keitel[1], Felipe V. Antolinez[1], Stefan Meyer[1], Raphael Brechbühler[1], Maria del Henar Rojo Sanz[1], David J. Norris[1]
[1] Optical Materials Engineering, D-MAVT, ETH Zurich

Light-emitting nanocrystals are highly attractive for novel lighting applications and quantum optics. To exploit their full potential, precise knowledge of their excitation and emission spectra as well as their underlying physical mechanism is crucial. Ensemble inhomogeneity washes out many phenomena such as fine-structure splitting, blinking, and spectral diffusion. Consequently, single-particle studies are pivotal to deepen the understanding. Over the past years, these studies have focused on measuring the emission lifetime and emission spectra of individual particles, which restricts extracted information to the lowest excited state. While excitation spectra can provide additional insight into higher excited states, they are inherently much more difficult to measure on single particles. A sequential probing of the different wavelengths is necessary to obtain spectral information and especially blinking thus obscures the single-particle excitation spectrum. We present a novel approach to measure excitation spectra based on a broadband light source and a rapidly tunable narrow filter. We perform repeated spectral excitation scans at rates above 100 Hz to average out effects of blinking. During our scans, we record not only the wavelength that caused the emission of specific photons but also the corresponding arrival times. We identify moments in time where the individual quantum dot was in a “bright” or in a “dim” state. The rapid scanning allows us then to extract the separate excitation spectra of transiently occurring states of the quantum emitter. We leverage this to gain further insight into the origin of blinking in CdSe/CdS/ZnS quantum dots that show multiple discrete dim states. We observe a bright, a grey, and a dark state that occur in the same quantum dot. We attribute the bright and the dark state to excitonic emission while the grey state shows a change in the excitation spectrum that we attribute to a trion state.

Thin Films & Mesoscopic Structures

Epitaxial Growth and Electrical Control of Antiferromagnetic Mn_2Au Films

Zhentao Liu[1,2], Zhaochu Luo[1,2], Simone Finizio[3], Kevin Hofhuis[1,2], Sergii Parchenko[1,2], Armin Kleibert[3], Pietro Gambardella[4], Laura J. Heyderman[1,2], Aleš Hrabec[1,2]
[1] Mesoscopic Systems, D-MATL, ETH Zurich and PSI
[2] Multiscale Materials Experiments, PSI
[3] Swiss Light Source, PSI
[4] Magnetism & Interface Physics, D-MATL, ETH Zurich

Having the advantages of immunity to external magnetic fields and fast spin dynamics, antiferromagnetic materials open a new door towards the next generation of high-speed data storage devices. Here, we optimized the growth conditions of epitaxial Mn_2Au thin films. The antiferromagnetic domain configuration of the films is directly mapped exploiting x-ray magnetic linear dichroism. The films are consequently patterned into star-shaped devices for electrical switching measurements. We observe a change of resistance, which implies current-induced switching of Néel vectors. The Néel vector switching offers a platform to investigate the microscopic mechanism of the magnetization dynamics.

Optical Fourier Surfaces

Nolan Lassaline[1], Raphael Brechbühler[1], Sander J.W. Vonk[1,2], Korneel Ridderbeek[1], Martin Spieser[3], Samuel Bisig[3], Boris le Feber[1], Freddy T. Rabouw[1,2], David J. Norris[1]
[1] Optical Materials Engineering D-MAVT, ETH Zurich
[2] Debye Institute for Nanomaterials Science, Utrecht University
[3] Heidelberg Instruments Nano/SwissLitho, Zurich

Gratings and holograms are patterned surfaces that tailor optical signals by diffraction. Despite their long history, variants with remarkable functionalities continue to be discovered. Further advances could exploit Fourier optics, which specifies the surface pattern that generates a desired diffracted output through its Fourier transform. To shape the optical wavefront, the ideal surface profile should contain a precise sum of sinusoidal waves, each with a well-defined amplitude, spatial frequency, and phase. However, because fabrication techniques typically yield profiles with at most a few depth levels, complex 'wavy' surfaces cannot be obtained, limiting the straightforward mathematical design and implementation of sophisticated diffractive optics. Here we present a simple yet powerful approach to eliminate this design–fabrication mismatch by demonstrating optical surfaces that contain an arbitrary number of specified sinusoids. We combine thermal scanning-probe lithography and templating to create periodic and aperiodic surface patterns with continuous depth control and subwavelength spatial resolution. Multicomponent linear gratings allow precise manipulation of electromagnetic signals through Fourier-spectrum engineering. Consequently, we overcome a previous limitation in photonics by creating an ultrathin grating that simultaneously couples red, green, and blue light at the same angle of incidence. More broadly, we analytically design and accurately replicate intricate two-dimensional moiré patterns, quasicrystals, and holograms demonstrating a variety of previously impossible diffractive surfaces. Therefore, this approach can provide benefit for optical devices (biosensors, lasers, metasurfaces, and modulators) and emerging topics in photonics (topological structures, transformation optics, and valleytronics) [1,2].

[1] N. Lassaline et al., Nature (accepted).
[2] N. Lassaline et al., arXiv:1912.09442.

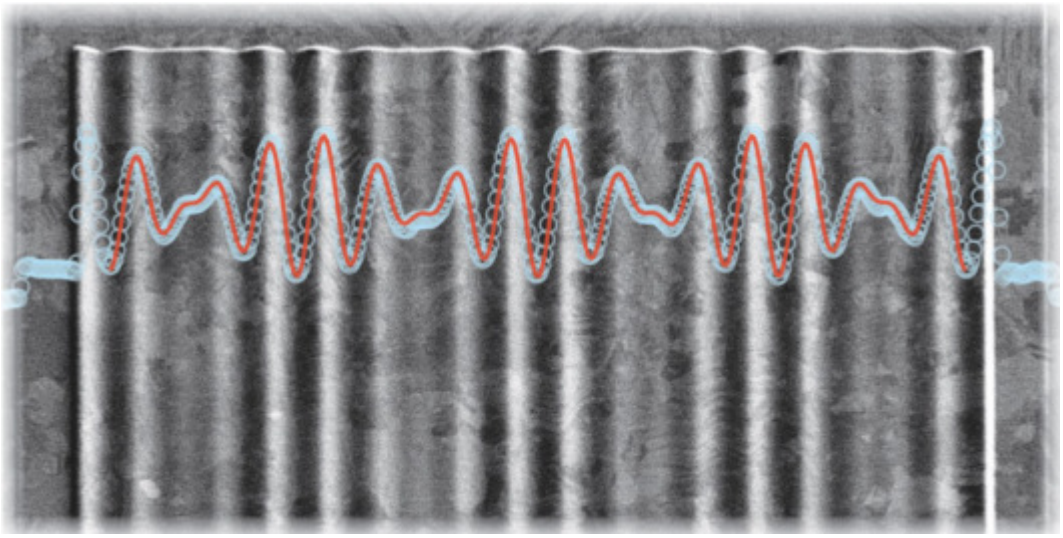

Fig.: Scanning electron micrograph of a wavy silver surface. The blue circles represent the measured surface profile, taken using atomic force microscopy. The red line shows the target profile, revealing an excellent match between the designed and fabricated surface.

Grain-size Tuning of VO_2 Films on Si Using Millisecond Flash Annealing

Elisabetta Corti[1,2], Joaquin Antonio Cornejo Jimenez[1,2], Federico Balduini[1], Kirsten Moselund[1], Bernd Gotsmann[1], Siegfried Karg[1]
[1] IBM Research Zurich
[2] NANOLAB, Personalized Health, EPF Lausanne

Due to its metal-to-insulator phase transition, VO_2 has been identified as a promising material for electronic device applications, spanning from implementation of efficient electrical and optical switches to oscillators, with a focus on neuromorphic computing with Oscillatory Neural Networks [1]. Envisioning these technological applications, the development of a material deposition process that results in high quality VO_2 films on a Silicon substrate is critical. VO_2 films deposition on Si/SiO_2 leads to crystallization of the VO_2 into rough, granular films [2]. The granularity of the film has been shown to have major impact on the reliability and variability of the devices [3]. In this work we explore a millisecond flash anneal technique to post-anneal VO_2 films deposited on Si/SiO_2 with atomic layer deposition (ALD). We demonstrate that flash lamp annealing, compared to a slower anneal process, allows for a fine tuning of the average grain size of the VO_2 film. This results in a smoother electrical transition in scaled electrical switches, with major improvements in single switch and oscillator device performances.

[1] A. Parihar et al. J. Appl. Phys. 117, 1 (2015).
[2] A.P. Peter et al, Adv. Funct. Mater. 25, 679 (2015).
[3] E. Corti, et al., Solid. State. Electron., 107729, (2019).

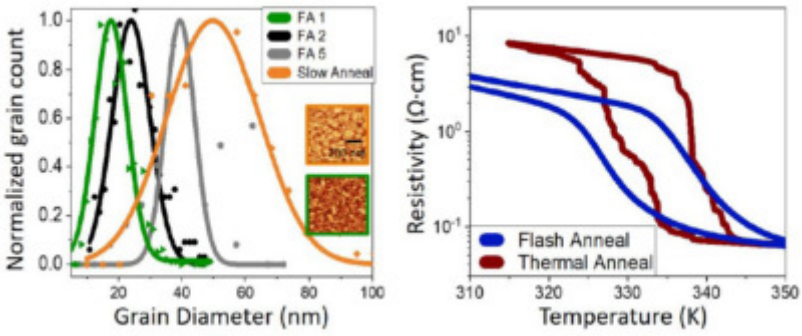

Fig.: Left: Average VO_2 grain dimension obtained with different flash annealing parameters. The characterization was performed through Atomic Force Microscopy images and post-processing. Right: comparison of the phase change hysteresis of a flash-annealed device compared to a slow-annealed device of the same dimensions.

ETH Zürich
Competence Center for Materials
and Processes (MaP)
Leopold-Ruzicka-Weg 4
HCP F 35.1
8093 Zurich

www.map.ethz.ch